Cooperation or Not? Strategic Responses to Imbalance Pricing under Multi-Source Uncertainty

Rongqing Yin[a], Yeming Dai[a,*], Mingming Leng[b]

[a] School of Business, Qingdao University, Qingdao, 266071, China
[b] Faculty of Business, Lingnan University, Hong Kong, China

Abstract

With growing variable renewable energy (VRE), electricity markets face supply–demand balancing under multi-source uncertainty, including generation fluctuations, supply interruptions, and load variability. Under imbalance pricing, decentralized decisions by a variable renewable energy generator (VREG) and an electricity retailer (ER) can amplify deviations and increase imbalance settlement costs. To examine the effectiveness of strategic coordination, we develop two-stage game-theoretic models for the day-ahead and real-time markets under single imbalance pricing, comparing a non-cooperative mechanism with a cooperative mechanism. Forecast deviations are represented by a symmetric Beta distribution so that prediction accuracy can be varied and analyzed systematically. The results show that the cooperative mechanism improves overall market performance: it increases supply-side profits and user welfare (thus raising social welfare) and reduces deviations and the likelihood of extreme imbalance settlements. At the same time, although the cooperative mechanism increases retail price volatility, it lowers the expected retail price and raises expected consumption relative to the non-cooperative mechanism. Moreover, cooperation weakens—but does not eliminate—the VREG's incentive to improve forecasting accuracy, because risk sharing lowers the marginal gain from additional accuracy improvements. A case study using data from Germany during the December 2024 "Dunkelflaute" shows that cooperation increases expected coalition profit by 3.4% while substantially mitigating extreme-loss risk. Finally, extensions with incomplete demand response and a flexible power generator (FPG) capacity constraint suggest that, under more realistic demand-side and flexibility limitations, the original model may underestimate the value of the cooperative mechanism.

Keywords: Multi-source uncertainties, Imbalance pricing, Stackelberg game, Cournot game, Cooperative game, Shapley value

* Corresponding author
Email address: yemingdai@163.com (Yeming Dai)

1. Introduction

With the large-scale integration of variable renewable energy (VRE) such as wind and photovoltaic power, modern power systems face growing challenges in maintaining supply-demand balance. Owing to their inherent weather dependence, VRE outputs exhibit persistent fluctuations and are prone to sudden interruptions. For example, during the 2021 winter storms in Texas, widespread wind power shutdowns occurred due to turbine icing. In the 2024 Dunkelflaute event, wind generation in the UK dropped to below 5% during peak hours [1]. Similarly, in 2025, Spain and Portugal experienced Europe's largest blackout in recent years, with high VRE penetration widely regarded as a major contributing factor [2]. At the same time, on the demand side, electricity consumption has also become increasingly volatile and difficult to forecast, driven by frequent extreme weather and unexpected events.

Above multi-source uncertainties introduce challenges not only for the system operator (SO) but also for market participants, such as variable renewable energy generator (VREG) and electricity retailer (ER).

For the SO, uncertainties substantially increase the complexity of system operation and dispatch. Specifically, these uncertainties often lead to discrepancies between day-ahead schedules and real-time conditions, resulting in frequent supply-demand imbalances. To reflect real-time system stress and allocate deviation responsibilities, SO implements imbalance pricing that penalizes market participants according to their contribution to these imbalances [3]. Imbalance pricing generally takes one of two forms: single imbalance pricing (SP), which applies the same price to positive and negative deviations, and dual imbalance pricing (DP), which distinguishes between positive and negative deviations with different prices. Compared to DP, SP is simpler, more transparent, and has become the dominant practice in liberalized electricity markets [4]. For instance, it is the default imbalance pricing in the European Union, which is widely recognized as the world's largest and most mature liberalized power market [5].

For market participants, these multi-source uncertainties induce significant revenue volatility, especially under extreme spot prices. To hedge against these risks, VREG and ER commonly sign long-term contracts (e.g., power purchase agreements and contracts for difference), which help stabilize expected revenues or procurement costs. However, while such contracts are effective in managing spot price volatility, they offer limited protection against deviation costs under imbalance pricing. This is because long-term contracts typically cover baseline volumes with stable expectations, while real-time deviations often fall outside the scope of such contracts and remain fully exposed to imbalance charges. In other words, these deviation risks persist—and may even intensify—despite existing long-term hedging instruments [6].

Moreover, deviation costs are shaped not only by external uncertainties. A crucial but often overlooked factor is the strategic decisions of market participants. Although VREG and ER are jointly exposed to deviation risks, they typically make decisions independently: the VREG focuses on minimizing penalties from delivery deviations, while the ER seeks to manage cost fluctuations through demand-side responses. Such separation of strategy can unintentionally amplify aggregate deviation risks and revenue instability for both sides.

Such decentralized decision-making gives rise to a natural question: Can strategic coordination between VREG and ER mitigate imbalance costs and improve economic outcomes? To explore this, we develop different two-stage game-theoretic models that capture interactions among VREG, ER, and users under imbalance pricing, comparing day-ahead trading decisions and real-time demand response strategies between cooperative and non-cooperative mechanisms. Furthermore, we incorporate forecast deviations into the framework using a symmetric Beta distribution, which allows us to examine how varying levels of prediction accuracy influence equilibrium strategies and the value of cooperation [7]. Specifically, this study aims to answer the following questions:

(1) How do cooperative and non-cooperative mechanisms affect the day-ahead and real-time strategies of VREG and ER?

(2) To what extent can cooperation mitigate imbalance risks and stabilize economic outcomes, and under what conditions does it yield significant benefits?

(3) How does VREG forecast accuracy influence strategic interactions and the value of coordination?

The remainder of this paper is organized as follows. Section 2 reviews the related literature; Section 3 introduces the market components and the two-stage structure; Section 4 formulates and solves the models under non-cooperative and cooperative mechanisms; Section 5 presents the equilibrium analysis and a case study; Section 6 extends the model to incorporate incomplete demand response and flexible power generator (FPG) capacity constraints; Section 7 summarizes the main findings and discusses managerial and policy implications as well as directions for future research.

2. Literature Review

This section reviews the literature along three key themes—multi-source uncertainties, imbalance pricing, and cooperative mechanism—reflecting our focus on how cooperation (relative to non-cooperation) shapes decisions and outcomes under imbalance pricing with multi-source uncertainty. We conclude by highlighting this study's contributions.

2.1. Multi-source Uncertainties

Existing studies widely emphasize the uncertainties in VRE output and the risks of supply interruptions, exploring their impacts on power system security and the behaviors of market participants. Al-Gwaiz et al. [8] and Aflaki & Netessine [9] investigate how the variability in VRE output influences traditional generators and market prices from the perspectives of market competition and investment incentives. Regarding extreme events and sudden interruptions, Gharehveran et al. [10], Lv et al. [11], and Ren et al. [12] propose optimization strategies from the viewpoints of microgrid resilience, integrated energy system flexibility, and storage configuration, respectively. Panahi et al. [13] incorporate partial and complete supply disruptions into supply chain design, introducing multi-source supply, multi-line transmission, and bypass routes to enhance system resilience. Feng et al. [14] and Xie et al. [15] further develop multi-stage stochastic optimization and stochastic-robust hybrid optimization models, respectively, incorporating flexible loads and hierarchical energy storage to strengthen the system's risk resilience.

On the demand side, load uncertainty is also a critical factor influencing power system operations. Parker et al. [16] highlight the challenges posed by load-side deviations for market design and policy formulation amid the energy transition. Lin et al. [17] propose an integrated optimization model considering user responses and multi-operator game, revealing the crucial role of demand-side flexibility in achieving supply-demand balance. Xie et al. [15] incorporate demand response into multi-uncertainty modeling for islanded energy systems, while Zhou et al. [18] leverage a variety of forecasting methods and peer-to-peer trading models to improve real-time supply-demand matching under uncertainty.

However, despite these advances, most studies treat VRE volatility, supply interruption risk, and demand uncertainty in isolation. A comprehensive framework that incorporates all three dimensions of uncertainty is still underdeveloped. To address this gap, this paper proposes an integrated modeling approach for multi-source uncertainty to systematically assess how the convergence of these uncertainties shapes supply-demand balance and market equilibrium outcomes.

2.2. Imbalance Pricing

Early studies such as Vandezande et al. [19] point out that a fair allocation of balancing costs is essential for integrating high shares of wind power. Van Der Veen et al. [20] demonstrate that SP effectively minimizes total imbalance costs by employing an agent-based simulation model. Empirical work by Bunn & Kermer [21] suggests that SP enhances market flexibility and reduces information lag under market reforms in the UK. Likewise, Shinde et al. [4] show that SP achieves optimal market efficiency in balancing market dispatch models with high renewable penetration. Ghiassi-Farrokhfal et al. [3] compared SP and DP and proposed an optimal SP to improve market adaptability.

Nevertheless, most studies focus on the design and efficiency of pricing mechanisms, with limited attention to how these rules influence strategic behaviors. Sunar & Birge [22] describe how similar commitment-penalty mechanisms shape the trading strategies of renewable generators under deviation risks. Clò & Fumagalli [23] and Yamujala et al. [24] primarily explore how different pricing mechanisms impact market behaviors and reserve capacity needs. Chen et al. [25] uncover the nonlinear relationship between imbalance prices and market volatility in the UK but offer limited insights into the specific behaviors of market participants within this framework.

What remains underexplored is how market participants — particularly VREG and ER — adjust their trading and demand response strategies under SP when facing deviation costs. To fill this gap, our study focuses on the behavioral dimension of imbalance pricing by modeling the strategic decisions of VREG and ER within two-stage game-theoretic frameworks.

2.3. Cooperative Mechanism

Cooperative mechanisms, as a crucial tool for coordinating the interests of multiple parties and managing uncertainties, have been widely studied in complex systems such as supply chain management and electricity markets. Cachon & Lariviere [26, 27] and Giri et al. [28] systematically examine how diversified cooperation can optimize supply chain collaboration and enhance overall performance. El Ouardighi & Kogan [29] extend cooperative mechanisms to dynamic quality management, analyzing how long-term cooperation enables supply chain members to improve product quality in a coordinated manner. Tang & Kouvelis [30] combine buyback and revenue-sharing contracts to reconcile the mismatch between suppliers' random output and retailers' flexible ordering strategies.

In electricity markets, Zhu et al. [31] reveal how cooperative mechanisms can improve grid integration of green electricity and achieve Pareto improvements under the dual uncertainties of renewable generation variability and market demand fluctuations. Zhu et al. [32] quantify the effects of competitive intensity and government subsidies on revenue-sharing ratios and profit allocation, highlighting the coordination function of cooperative mechanisms in complex market relationships. Kong et al. [33] argue from the perspective of government subsidies that, as renewable energy penetration and policy support increase, revenue-sharing mechanisms enhance adaptability and revenue stability in addressing demand fluctuations and supply-demand imbalances. Lei et al. [34] focus on vehicle-to-grid interactions and propose an optimal bidding strategy under revenue-sharing and uncertainty conditions, demonstrating how cooperative mechanisms can diversify risks, balance revenues, and strengthen system stability and adaptability in dynamic market environments.

Although previous studies have highlighted the benefits of cooperative mechanisms in multi-party collaboration and revenue optimization, their role in balancing supply-demand deviations is still underexplored. In response, this study examines how the cooperative mechanism affects strategic decision-making, deviation costs, and profit distribution between the VREG and the ER, compared with the non-cooperative mechanism.

2.4. Contributions

Based on the above literature review, this study makes four key contributions.

- **Uncertainties framework:** An integrated multi-source uncertainties framework is developed to jointly capture VRE output variability, supply interruption, and user load uncertainties, and to quantify their combined impact on supply-demand balance and market equilibrium.

- **Game-theoretic modelling:** Building on this multi-source uncertainties framework, we construct different two-stage game-theoretic models under the SP to capture the strategic interactions among VREG, ER, and users during both day-ahead commitments and real-time demand response.
- **Mechanism comparison:** By comparing cooperative and non-cooperative mechanisms, the study demonstrates the effectiveness of strategic coordination in mitigating deviation costs and stabilizing economic returns.
- **Distributional innovation:** Introducing the Beta distribution to model forecast deviations in VREG output effectively captures output fluctuations across varying levels of forecasting accuracy and generalizes the traditional assumption of a uniform distribution.

3. Market Components

This section presents the market's demand and supply structure, pricing mechanisms, and the decision-making sequence of market participants. We first describe the demand side in Section 3.1, then introduce the supply side and pricing mechanisms in Section 3.2. An overview of the two-stage market structure (day-ahead and real-time market) is provided in Section 3.3 (see Figure 2). For clarity, the notation used throughout the paper is summarized in Appendix A.

3.1. Demand

The total market demand is the aggregate consumption of N independent users. The welfare of user $i \in \{1, 2, \dots, N\}$ consists of three components: the utility derived from electricity consumption, the payment for electricity, and the dissatisfaction cost arising from deviations from the user's ideal consumption. It is given by

$$W_i(p_i, \hat{q}_i) = u_i(\hat{q}_i) - p_i\hat{q}_i - c_i(\hat{q}_i), \tag{1}$$

where p_i denotes the retail price and $\hat{q}_i$ represents the predicted consumption of user i. Due to demand uncertainty, the actual consumption of user i often deviates from the predicted value. To capture this deviation, a random disturbance term ε_i is introduced to model the prediction error, which is assumed to have zero mean and variance σ_i^2. This assumption implies that there is no systematic bias, while demand remains stochastic. Accordingly, the actual consumption of user i is given by $q_i = \hat{q}_i + \varepsilon_i$. Note that consumption throughout the paper refers to the user's metered net load, i.e., the net electricity exchanged with the ER, because under multi-source uncertainty it is the net load that directly affects the supply–demand balance.

The utility function $u_i(\hat{q}_i)$ satisfies the law of diminishing marginal utility. Following Li et al. [35] and Qu et al. [36], it is specified as

$$u_i(\hat{q}_i) = l_i \left(\hat{q}_i - \frac{1}{2\bar{q}_i}\hat{q}_i^2 \right), \tag{2}$$

where $l_i > 0$ denotes the utility intensity coefficient and $\bar{q}_i > 0$ represents the ideal consumption, i.e., the theoretical consumption that maximizes utility in the absence of cost considerations. In practice, due to electricity purchasing costs, the actual consumption is lower than the ideal consumption, i.e., $q_i < \bar{q}_i$. Consequently, the actual total demand $Q = \sum_{i=1}^{N} q_i$ is lower than the ideal total demand $\bar{Q} = \sum_{i=1}^{N} \bar{q}_i$.

The ER typically formulates purchase plans based on load predictions. However, these plans rarely coincide exactly with actual demand. Therefore, the ER may implement demand response to shift user loads. During this process, users may incur utility losses due to load reductions, which are modeled as dissatisfaction costs. Following Wen et al. [37], the dissatisfaction cost function is defined as

$$c_i(\hat{q}_i) = \frac{\eta_i}{2} \left(\bar{q}_i - \hat{q}_i\right)^2, \tag{3}$$

where $\eta_i > 0$ is the dissatisfaction sensitivity coefficient, reflecting the user's sensitivity to discomfort caused by load adjustments. Substituting Equations (2) and (3) into Equation (1), the welfare of user i can be rewritten as

$$W_i(p_i, \hat{q}_i) = l_i \left(\hat{q}_i - \frac{1}{2\bar{q}_i}\hat{q}_i^2\right) - p_i\hat{q}_i - \frac{\eta_i}{2} \left(\bar{q}_i - \hat{q}_i\right)^2. \tag{4}$$

Accordingly, user i faces the following optimization problem:

$$\max_{\hat{q}_i \in \Omega_i} \quad W_i(p_i, \hat{q}_i),$$

where $\Omega_i = \left\{\hat{q}_i \mid \hat{q}_i \in \mathbb{R},\ \underline{q}_i \leq \hat{q}_i \leq \bar{q}_i\right\}$ is the strategy set of user i, $\underline{q}_i$ denotes the minimum consumption of user i.

3.2. Supply and Pricing

Electricity is supplied by three types of generators: VREG, traditional energy generator (TEG), and FPG. This section introduces the key characteristics of each generator and explains the corresponding pricing mechanisms.

3.2.1. Uncertainty of VREG

The VREG, such as wind farms and solar photovoltaic plants, is highly dependent on weather conditions. As a result, its generation exhibits persistent fluctuations and is subject to sudden interruptions. The actual generation of VREG, denoted as $Q^{\mathrm{A}}_{\mathrm{VREG}}$, deviates from its predicted level $Q^{\mathrm{P}}_{\mathrm{VREG}} = \gamma\bar{Q}$, where γ represents the market share of VREG in the ideal total demand. Accordingly, it is specified as $Q^{\mathrm{A}}_{\mathrm{VREG}} = \xi\,\gamma\,\bar{Q}\,(1 + v)$, where $\xi \sim \text{Bernoulli}(\phi)$ represents the operational status of VREG: $\xi = 1$ with probability ϕ, indicating normal operation, and $\xi = 0$ with probability $1 - \phi$, indicating complete interruption. The variable $v \in [-\bar{v}, \bar{v}]$ is a continuous random variable that captures the deviation from the predicted generation under normal operation, where $\bar{v}$ denotes the maximum deviation.

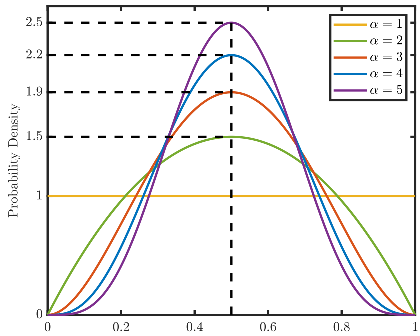

Figure 1: Symmetric Beta distributions with different parameters α

Existing studies often assume that v follows a uniform distribution, implying equal probability across all deviations. In practice, as prediction accuracy improves, deviations tend to concentrate within narrower ranges. To capture this feature, we adopt a symmetric Beta distribution, $\mathrm{Beta}(\alpha, \alpha)$, which generalizes the uniform distribution [7]. The distribution is defined on $[0, 1]$, with its shape governed by the parameter α. As shown in Figure 1, when $\alpha = 1$, it reduces to the uniform distribution. As α increases, the distribution becomes increasingly concentrated around the midpoint, reflecting higher prediction accuracy and stronger deviation control. This specification not only includes the uniform distribution as a special case, but also flexibly captures deviation performance under varying prediction accuracy levels. Moreover, its closed-form representation facilitates analytical derivations. To match the the practical deviation range, we construct the following affine transformation map the support to $[-\bar{v}, \bar{v}]$: $v = 2\bar{v}X - \bar{v}$, $X \sim \mathrm{Beta}(\alpha, \alpha)$. The probability density function of v is given by

$$f(v; \alpha) = \frac{1}{2\bar{v}B(\alpha, \alpha)} \left(\frac{\bar{v}^2 - v^2}{4\bar{v}^2} \right)^{\alpha - 1},$$

where $B(\alpha, \alpha) = \int_0^1 x^{\alpha-1}(1 - x)^{\alpha-1}\, \mathrm{d}x$ is the beta function. The mean and variance of v are $\mathbb{E}(v) = 0$, $\mathrm{Var}(v) = \bar{v}^2/(2\alpha + 1)$.

3.2.2. TEGs and Day-Ahead Clearing Pricing

TEGs refer to fossil-fuel-based generators such as coal- and oil-fired power plants. Due to their stable and controllable generation, TEGs are primarily deployed to meet the system's baseload demand. In contrast, VREG exhibits near-zero marginal generation costs and contributes to carbon emission reductions, and is therefore granted dispatch priority. We assume that even at its maximum output, VREG can not fully satisfy total electricity demand, i.e., $\gamma\bar{Q}(1 + \bar{v}) < \bar{Q}$. Consequently, the remaining demand must be supplied by TEGs.

Although electricity is typically supplied by multiple TEGs in practice, under perfect competition the day-ahead clearing price w^{DA} is determined by the marginal cost of the final unit supplied, regardless of the number of TEGs [38]. Therefore, without loss of generality, these TEGs can be equivalently represented as a single aggregated TEG. Influenced by fuel costs, its marginal cost increases linearly with generation at rate k_1 [3]. Accordingly, the day-ahead clearing price w^{DA} is expressed as $w^{\mathrm{DA}} = k_1 Q_{\mathrm{TEG}}$, where Q_{TEG} denotes the generation of the aggregated TEG.

3.2.3. FPG and Imbalance Pricing

FPGs refer to fast-response generators such as gas turbines, battery storage systems, and pumped hydro units. Owing to their ability to rapidly adjust generation, they compensate for supply–demand mismatches in the real-time market, thereby maintaining system balance.

To account for the additional costs of real-time balancing, the SO employs imbalance pricing to settle deviations between scheduled and actual quantities. Under the SP, all deviation (e.g., over-generation or shortages) are settled at a uniform price, usually set equal to the marginal generation cost of FPG [3]. Since FPG incurs higher operational costs than TEG, its marginal generation cost increases linearly with its generation at rate k_2, where $k_2 > k_1 > 0$. Accordingly, the imbalance price w^{IM} is expressed as $w^{\mathrm{IM}} = k_1 Q_{\mathrm{TEG}} + k_2 Q_{\mathrm{FPG}}$, where Q_{FPG} denotes the generation of FPG. When a supply surplus arises, FPG reduces generation or absorbs excess electricity, leading to a lower imbalance price, which signals other generators to scale back production. Conversely, under a supply shortage, FPG increases generation to fill the gap, raising the imbalance price and encouraging additional supply while discouraging consumption. For analytical tractability, we assume that FPG has sufficient flexibility to fully compensate real-time supply shortfalls, thereby avoiding involuntary load shedding.

3.3. Two-Stage Market Structure

This section examines the two-stage market structure, consisting of a day-ahead market and a real-time market. Figure 2 provides an overview of the market timeline. The subsequent subsections specify the operational rules and the sequence of decisions.

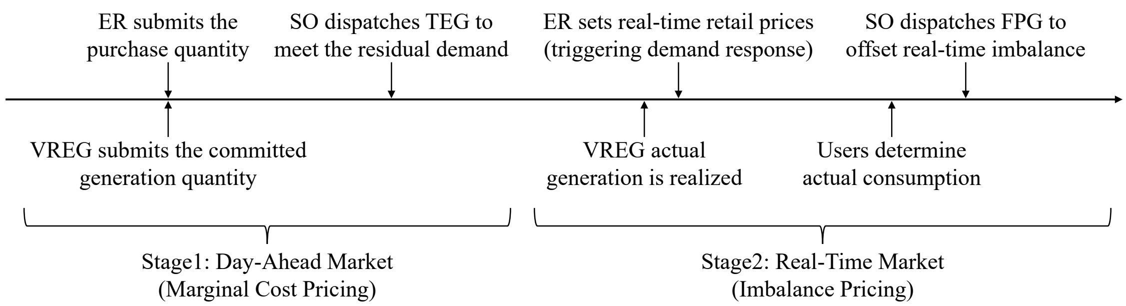

Figure 2: The Two-Stage Electricity Market Structure

3.3.1. Day-Ahead Market

The day-ahead market refers to the trading stage prior to the actual delivery of electricity. At this stage, market participants submit preliminary power schedules based on predicted information, thereby determining the market-clearing price and committing most supply and demand in advance.

Specifically, the ER submits a day-ahead purchase quantity to the SO based on its demand forecast, denoted by $Q_{\mathrm{ER}}^{\mathrm{DA}} = \theta\bar{Q}$, where θ represents the purchasing proportion relative to the ideal total demand $\bar{Q}$. Meanwhile, the VREG submits a day-ahead committed generation quantity to the SO based on its forecasted output. It is specified as $Q_{\mathrm{VREG}}^{\mathrm{C}} = Q_{\mathrm{VREG}}^{\mathrm{P}}(1+d) = \gamma\bar{Q}(1+d)$, where d represents the commitment adjustment relative to the predicted generation. Given generation uncertainty of VREG, the committed quantity is bounded by the maximum feasible output, $\gamma\bar{Q}(1+d) \leq \gamma\bar{Q}(1+\bar{v})$, which implies that $d \in [-1, \bar{v}]$.

After receiving the day-ahead schedules from both the ER and the VREG, the SO allocates the remaining generation requirement to the TEG as $Q_{\mathrm{TEG}} = \theta\bar{Q} - Q_{\mathrm{VREG}}^{\mathrm{C}}$. The TEG does not make strategic decisions; its generation is determined passively by the SO to ensure system balance. Finally, all supply-side participants are settled at the marginal cost price w^{DA}.

3.3.2. Real-Time Market

The real-time market corresponds to the stage of actual electricity delivery. Its primary role is to correct deviations between day-ahead schedules and real-time conditions, thereby restoring supply–demand balance.

At this stage, the actual generation of VREG, denoted as $Q_{\mathrm{VREG}}^{\mathrm{A}}$, is realized. It may differ from the committed generation $Q_{\mathrm{VREG}}^{\mathrm{C}}$, leading to a generation deviation: $\Delta Q_{\mathrm{VREG}} = Q_{\mathrm{VREG}}^{\mathrm{A}} - Q_{\mathrm{VREG}}^{\mathrm{C}}$. If $\Delta Q_{\mathrm{VREG}} < 0$, VREG's actual generation falls short of its commitment, creating a supply deficit. Conversely, if $\Delta Q_{\mathrm{VREG}} > 0$, excess generation must be absorbed by the system.

Similarly, the actual total consumption of users Q may differs from the day-ahead purchase plan $Q_{\mathrm{ER}}^{\mathrm{DA}} = \theta\bar{Q}$, resulting in a consumption deviation $\Delta Q_{\mathrm{ER}} = \theta\bar{Q} - Q$. To reduce imbalance costs, the ER implements demand response by adjusting retail prices to influence user consumption. If $\Delta Q_{\mathrm{ER}} < 0$ (i.e., a purchase shortfall), the ER raises prices to curb demand. If $\Delta Q_{\mathrm{ER}} > 0$ (i.e., a purchase surplus), the ER lowers prices to stimulate consumption.

Demand response alone may not fully eliminate the supply–demand imbalance. Therefore, the SO dispatches the FPG to quickly adjust its output and compensate for the remaining supply–demand gap. The resulting FPG generation is $Q_{\mathrm{FPG}} = Q - S^{\mathrm{A}}$, where $S^{\mathrm{A}} = Q_{\mathrm{VREG}}^{\mathrm{A}} + Q_{\mathrm{TEG}}$ denotes the actual total electricity supply. If $Q > S^{\mathrm{A}}$, the FPG provides additional generation to cover the deficit; otherwise, it absorbs surplus supply. Finally, all supply-side participants settle their deviations at the imbalance price w^{IM}.

4. Model Formulation and Solution

4.1. Non-Cooperative Mechanism

To capture the strategic behaviors of market participants under multi-source uncertainty, this section develops and analyzes a two-stage non-cooperative game model involving the ER, VREG, and users: the VREG and the ER engage in a Cournot game in the day-ahead stage; the ER and users interact in a Stackelberg game in the real-time stage. Since the decisions in the day-ahead stage are influenced by the decision in the real-time stage, the model is solved using the backward induction method.

4.1.1. Model Formulation

In the day-ahead stage, the ER and the VREG independently determine their respective purchase ratio θ and commitment adjustment d to maximize their own expected profits. Their strategic interaction is formulated as the following Cournot game:

$$\begin{cases} \max\limits_{\theta \in \Omega_\theta} \ \mathbb{E}\left[\pi^{\mathrm{DA}}_{\mathrm{ER,NC}}(\theta, d, \boldsymbol{p}^*, \boldsymbol{q}^*)\right], \\ \max\limits_{d \in \Omega_d} \ \mathbb{E}\left[\pi^{\mathrm{DA}}_{\mathrm{VREG,NC}}(\theta, d, \boldsymbol{p}^*, \boldsymbol{q}^*)\right], \end{cases} \tag{5}$$

where $\pi^{\mathrm{DA}}_{\mathrm{ER,NC}}$ and $\pi^{\mathrm{DA}}_{\mathrm{VREG,NC}}$ denote the day-ahead profits of the ER and VREG under the non-cooperative mechanism. The strategy set for ER is $\Omega_\theta = \left\{\theta \,\middle|\, \theta \in \mathbb{R},\ (Q_{\min}/\bar{Q}) \le \theta \le 1\right\}$, where $Q_{\min} = \sum_{i=1}^{N} \underline{q}_i$ denotes the aggregate minimum demand on the user side. The lower bound ensures that the ER procures at least the electricity required to satisfy users' minimum demand. The strategy set for VREG is $\Omega_d = \{d \mid d \in \mathbb{R},\ -1 \le d \le \bar{v}\}$.

In the real-time stage, the ER acts as the leader, setting the retail prices to maximize its expected profit, while users act as followers, adjusting their consumption q_i to maximize individual welfare. This interaction is formulated as the following Stackelberg game:

$$\begin{cases} \max\limits_{p \in \Omega_p} \ \mathbb{E}_\varepsilon\left[\pi^{\mathrm{RT}}_{\mathrm{ER,NC}}(\theta^*, d^*, \boldsymbol{p}, \boldsymbol{q}^*(\boldsymbol{p}))\right], \\ \text{s.t.} \quad q_i^*(p_i) = \arg\max\limits_{q_i \in \Omega_i} W_i(q_i, p_i), \qquad \forall i = 1, \dots, N, \end{cases} \tag{6}$$

where $\pi^{\mathrm{RT}}_{\mathrm{ER,NC}}$ represents the profit of ER in the real-time stage under the non-cooperative mechanism. The feasible price set for ER is $\Omega_{\mathbf{p}} = \{\boldsymbol{p} = (p_1, \dots, p_N) \mid p_i \in \mathbb{R},\ 0 < p_i < \bar{p}_i,\ \forall i = 1, \dots, N\}$, where $\bar{p}_i$ is the maximum price for user i. The feasible consumption set for user i is $\Omega_i = \left\{q_i \mid q_i \in \mathbb{R},\ \underline{q}_i \le q_i \le \bar{q}_i\right\}$.

4.1.2. Model Solution

In the real-time stage, the ER adjusts electricity prices to implement demand response, aiming to reduce imbalance costs caused by deviations between the day-ahead procurement plan and actual user consumption. The ER's profit function in the real-time stage consists of two components: revenue from user payments and imbalance settlement costs, expressed as

$$\pi^{\mathrm{RT}}_{\mathrm{ER,NC}} = \sum_{i=1}^{N} p_i q_i + w^{\mathrm{IM}} \Delta Q_{\mathrm{ER}}.$$

Taking the expectation over $\boldsymbol{\varepsilon}$ yields

$$\begin{aligned}\mathbb{E}_{\varepsilon}\left(\pi^{\mathrm{RT}}_{\mathrm{ER,NC}}\right) = {} & \sum_{i=1}^{N} p_i \hat{q}_i + k_2 \left(\sum_{i=1}^{N} \hat{q}_i - \theta \bar{Q} + Q^{\mathrm{C}}_{\mathrm{VREG}} - Q^{\mathrm{A}}_{\mathrm{VREG}} \right) \left(\theta \bar{Q} - \sum_{i=1}^{N} \hat{q}_i \right) \\ & + k_1 \left(\theta \bar{Q} - Q^{\mathrm{C}}_{\mathrm{VREG}} \right) \left(\theta \bar{Q} - \sum_{i=1}^{N} \hat{q}_i \right) - k_2 \sum_{i=1}^{N} \sigma_i^2.\end{aligned} \tag{7}$$

By substituting Equations (4) and (7) into Equation (6) and further solving, we obtain Theorem 1 as follows.

Theorem 1. *Under the non-cooperative mechanism, the Stackelberg game between the ER and users has the unique equilibrium solution* $(\boldsymbol{p}^*_{\mathrm{NC}}, \boldsymbol{q}^*_{\mathrm{NC}})$*, given by*

$$p^*_{i,\mathrm{NC}} = \frac{1}{2b_i} + \frac{k_1(\theta\bar{Q} - Q^{C}_{VREG}) - k_2(2\theta\bar{Q} - \bar{Q}) - k_2(Q^{\mathrm{A}}_{\mathrm{VREG}} - Q^{\mathrm{C}}_{\mathrm{VREG}})}{2(k_2\Lambda + 1)}, \tag{8}$$

$$q^*_{i,\mathrm{NC}} = \bar{q}_i \left(1 - b_i p^*_{i,\mathrm{NC}}\right) + \varepsilon_i, \tag{9}$$

where $b_i = 1/(\eta_i \bar{q}_i + l_i)$ *and* $\Lambda = \sum_{i=1}^{N} b_i \bar{q}_i$.

Proof. See Appendix B.

In the day-ahead stage, the ER's profit function consists of three components: the revenue from user payments for electricity consumption, the purchasing cost in the day-ahead market, and the imbalance cost caused by real-time deviations. This function can be expressed as

$$\pi^{\mathrm{DA}}_{\mathrm{ER,NC}} = \sum_{i=1}^{N} p_i q_i - w^{\mathrm{DA}} \theta \bar{Q} + w^{\mathrm{IM}} \Delta Q_{\mathrm{ER}}. \tag{10}$$

By substituting Equations (8) and (9) into Equation (10) and subsequently taking the full expectation, we derive the ER's expected profit function as

$$\begin{aligned}\mathbb{E}\left(\pi^{\mathrm{DA}}_{\mathrm{ER,NC}}\right) = \frac{1}{4(k_2\Lambda + 1)} \Big\{ & - A\theta^2\bar{Q}^2 - 2B\theta\bar{Q}^2 + 2DQ^{\mathrm{C}}_{\mathrm{VREG}}\theta\bar{Q} + {Q^{\mathrm{C}}_{\mathrm{VREG}}}^2 (k_2 - k_1)^2 \Lambda \\ & - 2\bar{Q}Q^{\mathrm{C}}_{\mathrm{VREG}}(k_2 - k_1)(k_2\phi\gamma\Lambda + 1) + \phi k_2^2 \gamma^2 \bar{Q}^2 \Lambda \left[1 + \mathrm{Var}(v)\right] \\ & + (k_2\Lambda + 1)\Big(\sum_{i=1}^{N} \frac{\bar{q}_i}{b_i} - 4k_2 \sum_{i=1}^{N} \sigma_i^2 \Big) + (2\phi\gamma - 1)k_2\bar{Q}^2 \Big\},\end{aligned} \tag{11}$$

where $A = k_1(4k_2 - k_1)\Lambda + 4k_2$, $B = k_2\phi\gamma(k_1\Lambda + 2) - (2k_2 - k_1)$, $D = k_1(3k_2 - k_1)\Lambda + 2k_2$.

The profit function of the VREG in the day-ahead stage consists of the revenue from electricity sales and the imbalance cost, which is expressed as

$$\pi^{\mathrm{DA}}_{\mathrm{VREG,NC}} = w^{\mathrm{DA}} Q^{\mathrm{C}}_{\mathrm{VREG}} + w^{\mathrm{IM}} \Delta Q_{\mathrm{VREG}}. \tag{12}$$

Substituting Equations (8) and (9) into Equation (12) and taking expectations, we obtain the VREG's expected day-ahead profit as

$$\begin{aligned} \mathbb{E}\big(\pi^{\mathrm{DA}}_{\mathrm{VREG,NC}}\big) = \frac{1}{2(k_2\Lambda + 1)} \Big\{ &(F + k_2\theta G)\bar{Q}Q^{\mathrm{C}}_{\mathrm{VREG}} - k_2 H {Q^{\mathrm{C}}_{\mathrm{VREG}}}^2 + k_2\phi\gamma\bar{Q}^2(1 - 2\theta) \\ &+ \phi\gamma\bar{Q}^2(k_2\Lambda + 2)\big[k_1\theta - k_2\gamma - k_2\gamma \mathrm{Var}(v)\big] \Big\}, \end{aligned} \tag{13}$$

where $F = \phi\gamma(2k_2 - k_1)(k_2\Lambda + 2) - k_2$, $G = k_1\Lambda + 2$, $H = (k_1 + k_2)\Lambda + 2$. Combining Equations (11) and (13) with the game problem in Equation (5) and solving for equilibrium yields Theorem 2.

Theorem 2. *Under the non-cooperative mechanism, the Cournot game between the ER and the VREG has the unique equilibrium solution* $(\theta^*_{\mathrm{NC}}, d^*_{\mathrm{NC}})$*, given by*

$$\theta^*_{\mathrm{NC}} = \frac{DF - 2k_2BH}{k_2(2AH - DG)}, \tag{14}$$

$$d^*_{\mathrm{NC}} = \frac{AF - k_2BG}{\gamma k_2(2AH - DG)} - 1. \tag{15}$$

Proof. See Appendix C.

4.2. Cooperative Mechanism

Under the cooperative mechanism, the ER and the VREG form a coalition to jointly bear market risks and collaboratively optimize both day-ahead trading strategies and real-time demand response. The primary objective is to enhance overall profitability and reduce imbalance costs. In contrast to the non-cooperative mechanism, where the ER and the VREG act independently, the coalition makes unified decisions in the day-ahead stage. In the real-time stage, the coalition and users engage in a Stackelberg game. Internally, profit allocation within the coalition is modeled as a cooperative game, with profits allocated based on the Shapley value. Since the coalition's profit allocation must be agreed upon in advance, and the day-ahead decisions influence the real-time equilibrium outcomes, a backward induction approach is adopted. Specifically, the model first solves the real-time stage, then traces back to the day-ahead stage, and finally determines the internal profit allocation scheme.

4.2.1. Model Formulation

In the day-ahead stage, the coalition jointly determines the purchase ratio θ and commitment adjustment d to maximize its total expected profit. The resulting optimization problem is formulated as follows:

$$\max_{(\theta,d)\in(\Omega_\theta,\Omega_d)} \mathbb{E}\left[\pi^{\mathrm{DA}}_{\mathrm{Coa,C}}(\theta, d, \boldsymbol{p}^*, \boldsymbol{q}^*)\right], \tag{16}$$

where $\pi^{\mathrm{DA}}_{\mathrm{Coa,C}}$ represents the day-ahead profit of the coalition under the cooperative mechanism.

In the real-time stage, the coalition acts as the leader by determining electricity prices to maximize its expected profit, while the users, as followers, optimize their consumption to maximize their welfare. This strategic interaction is formulated as the following Stackelberg game:

$$\begin{cases} \max\limits_{p\in\Omega_p} \mathbb{E}_\varepsilon\left[\pi^{\mathrm{RT}}_{\mathrm{Coa,C}}(\theta^*, d^*, \boldsymbol{p}, \boldsymbol{q}^*(p))\right], \\ \text{s.t.} \quad q_i^*(p_i) = \arg\max\limits_{q_i\in\Omega_i} W_i(q_i, p_i), \qquad \forall i = 1, \dots, N. \end{cases} \tag{17}$$

where $\pi^{\mathrm{RT}}_{\mathrm{Coa,C}}$ represents the real-time profit of the coalition under the cooperative mechanism.

4.2.2. Model Solution

In the real-time stage, the coalition implements demand response by adjusting electricity prices to reduce imbalance costs resulting from deviations between day-ahead decisions and actual electricity demand. The coalition's profit function in the real-time stage consists of two components: revenue from user payments and imbalance settlement costs. This function is expressed as follows:

$$\pi^{\mathrm{RT}}_{\mathrm{Coa,C}} = \sum_{i=1}^{N} p_i q_i + w^{\mathrm{IM}}\big(\Delta Q_{\mathrm{ER}} + \Delta Q_{\mathrm{VREG}}\big).$$

Taking the expectation over ε yields

$$\begin{aligned} \mathbb{E}_\varepsilon(\pi^{\mathrm{RT}}_{\mathrm{Coa,C}}) = {} & \sum_{i=1}^{N} p_i \hat{q}_i + k_1(\theta\bar{Q} - Q^{\mathrm{C}}_{\mathrm{VREG}})\Big(\theta\bar{Q} - \sum_{i=1}^{N}\hat{q}_i + Q^{\mathrm{A}}_{\mathrm{VREG}} - Q^{\mathrm{C}}_{\mathrm{VREG}}\Big) \\ & - k_2\Big(\theta\bar{Q} - \sum_{i=1}^{N}\hat{q}_i + Q^{\mathrm{A}}_{\mathrm{VREG}} - Q^{\mathrm{C}}_{\mathrm{VREG}}\Big)^2 - k_2\sum_{i=1}^{N}\sigma_i^2. \end{aligned} \tag{18}$$

By substituting Equations (4) and (18) into Equation (17) and further solving, we obtain Theorem 3 as follows.

Theorem 3. *Under the cooperative mechanism, the Stackelberg game between the coalition and users has the unique equilibrium solution* $(\boldsymbol{p}^*_{\mathrm{C}}, \boldsymbol{q}^*_{\mathrm{C}})$*, given by*

$$p^*_{i,\mathrm{C}} = \frac{1}{2b_i} + \frac{k_1(\theta\bar{Q} - Q^{C}_{VREG}) - k_2(2\theta\bar{Q} - \bar{Q}) - 2k_2(Q^{\mathrm{A}}_{\mathrm{VREG}} - Q^{\mathrm{C}}_{\mathrm{VREG}})}{2(k_2\Lambda + 1)}, \tag{19}$$

$$q_{i,\mathrm{C}}^{*} = \bar{q}_i\big(1 - b_i p_{i,\mathrm{C}}^{*}\big) + \varepsilon_i. \tag{20}$$

Proof. See Appendix D.

In the day-ahead market, the coalition's profit function consists of three components: the revenue from user payments for electricity consumption, the purchasing cost in the day-ahead market, and the imbalance cost caused by real-time deviations. The profit function can be expressed as

$$\pi_{\mathrm{Coa,C}}^{\mathrm{DA}} = \sum_{i=1}^{N} p_i q_i - w^{\mathrm{DA}}(\theta\bar{Q} - Q_{\mathrm{VREG}}^{\mathrm{C}}) + w^{\mathrm{IM}}\Delta Q_{\mathrm{VREG}} + w^{\mathrm{IM}}\Delta Q_{\mathrm{ER}}. \tag{21}$$

By substituting Equations (19) and (20) into Equation (21), and subsequently taking the full expectation, we derive the coalition's expected profit function as

$$\begin{aligned}\mathbb{E}\big(\pi_{\mathrm{Coa,C}}^{\mathrm{DA}}\big) = \frac{1}{4(k_2\Lambda+1)}\Big\{&2\bar{Q}(2k_2-k_1)(1-2\phi\gamma) - A\big(\theta\bar{Q} - Q_{\mathrm{VREG}}^{\mathrm{C}}\big)^2\big(\theta\bar{Q} - Q_{\mathrm{VREG}}^{\mathrm{C}}\big)\\ &- 4\phi k_2\gamma^2\bar{Q}^2\big[1+\mathrm{Var}(v)\big] + (k_2\Lambda+1)\big(\sum_{i=1}^{N}\frac{\bar{q}_i}{b_i} - 4k_2\sum_{i=1}^{N}\sigma_i^2\big)\\ &+ (4\phi\gamma-1)k_2\bar{Q}^2\Big\}.\end{aligned} \tag{22}$$

By substituting Equation (22) into Equation (16) and further solving, we obtain Theorem 4 as follows.

Theorem 4. *Under the cooperative mechanism, if $\gamma < \frac{1}{2\phi}$, then the optimal day-ahead decisions of the coalition, represented by $(\theta_{\mathrm{C}}^{*}, d_{\mathrm{C}}^{*})$, satisfy*

$$\theta_{\mathrm{C}}^{*} = \gamma(1+d_{\mathrm{C}}^{*}) + \frac{(2k_2-k_1)(1-2\phi\gamma)}{k_1(4k_2-k_1)\Lambda + 4k_2}.$$

Proof. See Appendix E.

4.2.3. Profit Allocation

To ensure sustainable cooperation, a fair and rational profit allocation mechanism is essential. This study adopts the Shapley value method, which allocates profits based on each member's marginal contribution. Let S denote any subset of the player set $\{\mathrm{ER}, \mathrm{VREG}\}$. The characteristic function $V(S)$ of the two-player coalition game $(\{\mathrm{ER}, \mathrm{VREG}\}, V)$ is defined as

$$V(S) = \begin{cases} \mathbb{E}^{*}(\pi_{\mathrm{Coa,C}}^{\mathrm{DA}}), & S = \{\mathrm{ER}, \mathrm{VREG}\},\\ \mathbb{E}^{*}(\pi_{\mathrm{ER,NC}}^{\mathrm{DA}}), & S = \{\mathrm{ER}\},\\ \mathbb{E}^{*}(\pi_{\mathrm{VREG,NC}}^{\mathrm{DA}}), & S = \{\mathrm{VREG}\},\\ 0, & S = \varnothing, \end{cases}$$

where $\mathbb{E}^*(\pi^{\mathrm{DA}}_{\mathrm{Coa,C}})$ represents the coalition's optimal expected profit under the cooperative mechanism, and $\mathbb{E}^*(\pi^{\mathrm{DA}}_{\mathrm{VREG,NC}})$ and $\mathbb{E}^*(\pi^{\mathrm{DA}}_{\mathrm{ER,NC}})$ are the optimal expected profits of the VREG and the ER, respectively, under the non-cooperative mechanism. The validity of the Shapley value allocation relies on whether the characteristic function $V(S)$ satisfies superadditivity [39], defined as follows.

Theorem 5. *The characteristic function $V(S)$ is superadditive, that is, for any disjoint subsets $S_1, S_2 \subseteq \{\mathrm{ER}, \mathrm{VREG}\}$, $V(S_1 \cup S_2) \geq V(S_1) + V(S_2)$.*

Proof. See Appendix F.

This property guarantees that the profit of the coalition is at least as large as the sum of the profits each participant individually: $V(\{\mathrm{ER}, \mathrm{VREG}\}) \geq V(\{\mathrm{ER}\}) + V(\{\mathrm{VREG}\})$. This ensures the economic feasibility of cooperation and provides incentives for the stable formation of a coalition. Accordingly, the coalition's profit can be reasonably allocated through the Shapley value, which is defined as

$$\mathbb{E}^*\left(\pi^{\mathrm{DA}}_{\mathrm{j,C}}\right) = \sum_{S \subseteq \{\mathrm{ER},\mathrm{VREG}\} \setminus \{j\}} \frac{|S|!\,(2-|S|-1)!}{2!}\left[V(S \cup \{j\}) - V(S)\right], \tag{23}$$

where $j \in \{\mathrm{ER}, \mathrm{VREG}\}$. In this study's two-player cooperative game setting, Equation (23) can be further simplified as

$$\mathbb{E}^*\left(\pi^{\mathrm{DA}}_{\mathrm{VREG,C}}\right) = V(\{\mathrm{VREG}\}) + \frac{1}{2}\left[V(\{\mathrm{VREG}, \mathrm{ER}\}) - V(\{\mathrm{VREG}\}) - V(\{\mathrm{ER}\})\right],$$

$$\mathbb{E}^*\left(\pi^{\mathrm{DA}}_{\mathrm{ER,C}}\right) = V(\{\mathrm{ER}\}) + \frac{1}{2}\left[V(\{\mathrm{VREG}, \mathrm{ER}\}) - V(\{\mathrm{VREG}\}) - V(\{\mathrm{ER}\})\right].$$

These equations show that profit allocation considers both the surplus generated through cooperation and the independent performance of each member. This ensures that each member receives a return aligned with its marginal contribution, thereby strengthening coalition stability.

5. Result Analysis

5.1. Equilibrium Analysis

This section presents a comparative analysis of the equilibrium solutions under both non-cooperative and cooperative mechanisms, aiming to evaluate how cooperation influences revenue stability and deviation cost control. Furthermore, sensitivity analyses are conducted to explore the impact of key parameters—such as generation uncertainty, supply interruption risk, predicting accuracy, and demand elasticity—on strategic decisions of market participants and the overall operational performance of the system.

Proposition 1. *When the day-ahead market reaches equilibrium, given the same purchase ratio*

$\theta_{\mathrm{C}}^* = \theta_{\mathrm{NC}}^*$, *the optimal commitment adjustment differ between the two mechanisms as follows:*

$$\text{(1) If } 0 < \gamma < \frac{k_1\Lambda + 2}{2\phi(k_1\Lambda + 1)\big[(4k_2 - k_1)\Lambda + 2\big]}, \text{ then } d_{\mathrm{C}}^* > d_{\mathrm{NC}}^*;$$

$$\text{(2) If } \frac{k_1\Lambda + 2}{2\phi(k_1\Lambda + 1)\big[(4k_2 - k_1)\Lambda + 2\big]} < \gamma < \frac{1}{2\phi}, \text{ then } d_{\mathrm{C}}^* < d_{\mathrm{NC}}^*.$$

Proof. See Appendix G.

Proposition 1 shows that the incentive effect of the cooperative mechanism depends on VREG's market share. As illustrated in Figure 3, when γ is small, VREG accounts for only a limited portion of supply, and its impact on the system's supply–demand balance is minor. In this case, the revenue-sharing rule of the cooperative mechanism incentivizes VREG to commit more generation, since imbalance costs are shared within the coalition. When γ is larger, VREG's generation uncertainty has a stronger impact on the system's balance, exposing it to higher imbalance costs. Under these conditions, the cooperative mechanism enables VREG to adopt more conservative strategies to manage risks without reducing profitability. In addition, Figure 3 reveals that as the imbalance penalty intensity increases (i.e., as k_2/k_1 becomes larger), the region in which $d_{\mathrm{C}}^* > d_{\mathrm{NC}}^*$ gradually shrinks. This indicates that stronger imbalance penalties make the coalition more cautious in committing generation.

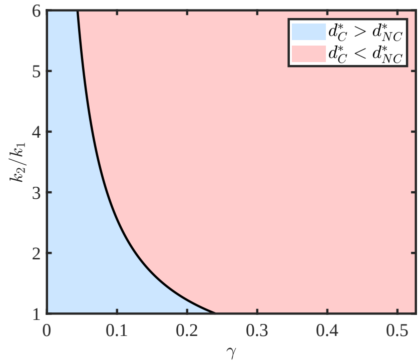

Figure 3: Comparison of d_{C}^* and d_{NC}^*

Proposition 2. *When the day-ahead market reaches equilibrium, the impact of the non-interruption probability ϕ on the purchase ratios and commitment adjustments under both mechanisms satisfies* *the following relationships:*

(1) *There exist thresholds* λ_1 *and* λ_2 *such that if* $\dfrac{k_2}{k_1} > \lambda_1$ *and* $\Lambda > \lambda_2$, *then* $\dfrac{\partial \theta^*_{\mathrm{NC}}}{\partial \phi} > 0$, *otherwise,* $\dfrac{\partial \theta^*_{\mathrm{NC}}}{\partial \phi} \leq 0$;

(2) *It always holds that* $\dfrac{\partial d^*_{\mathrm{NC}}}{\partial \phi} > 0$, *and for any fixed* θ^*_{C}, $\dfrac{\partial d^*_{\mathrm{C}}}{\partial \phi} > 0$.

Proof. See Appendix H.

As Proposition 2(1) shows, the monotonicity of θ^*_{NC} with respect to ϕ depends on two conditions: the imbalance pricing penalty must be sufficiently strong, and the average demand elasticity must exceed a critical threshold. When these conditions are met, θ^*_{NC} is positively correlated with the non-interruption probability ϕ, meaning that a higher ϕ leads the ER to procure a larger purchase ratio in the day-ahead market. Intuitively, stronger imbalance penalties and greater price sensitivity make the ER more inclined to secure demand through forward purchases as system reliability improves. Proposition 2(2) indicates that under the non-cooperative mechanism, the VREG's optimal commitment adjustment d^*_{NC} increases with the non-interruption probability ϕ. As generation becomes more reliable, the VREG faces lower imbalance risk and is therefore willing to commit more generation in the day-ahead market. Under the cooperative mechanism, for any fixed purchase ratio θ^*_{C}, the coalition's optimal commitment adjustment d^*_{C} also increases with ϕ. This reflects the fact that higher generation reliability encourages the coalition, like the VREG in the non-cooperative case, to commit more generation in advance.

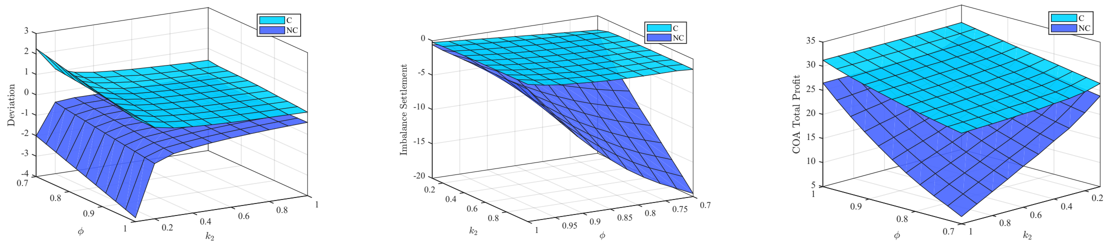

(a) Deviation Volume (b) Imbalance Settlement (c) COA Total Profit

Figure 4: Impacts of Imbalance Penalty Intensity and Interruption Probability on Market Outcomes

Based on the parameter settings in Ghiassi-Farrokhfal et al. [3] and Ito & Reguant [40], we conduct numerical simulations and obtain Figure 4. The results show that as k_2 increases, system deviations are significantly reduced, and market participants make more robust commitments in the day-ahead stage. However, when k_2 increases further, the marginal reduction in deviations becomes weaker and gradually stabilizes. This indicates that the remaining deviations are mainly driven by objective uncertainty rather than strategic decision-making. In this case, further increasing k_2 no longer improves supply–demand matching. Instead, it enlarges the scale of imbalance settlements, compresses supply-side profit margins, and increases the economic burden on market participants. This effect becomes more pronounced when ϕ is small. By contrast, the cooperative mechanism significantly restrains the scale of imbalance settlements. Even under high penalty intensity and high interruption risk, cooperation mechanism effectively mitigates risk exposure and stabilizes the profit structure, making it more advantageous than non-cooperation mechanism.

Proposition 3. *The effects of supply-side uncertainty on real-time stage equilibrium decisions under both non-cooperative and cooperative mechanisms satisfy the following properties.*

(1) With respect to supply interruption ξ,

$$\frac{\partial p_{i,\mathrm{C}}^{*}}{\partial \xi} = 2\,\frac{\partial p_{i,\mathrm{NC}}^{*}}{\partial \xi} < 0, \qquad \frac{\partial q_{i,\mathrm{C}}^{*}}{\partial \xi} = 2\,\frac{\partial q_{i,\mathrm{NC}}^{*}}{\partial \xi} > 0.$$

(2) With respect to VREG output deviation v,

$$\frac{\partial p_{i,\mathrm{C}}^{*}}{\partial v} = 2\,\frac{\partial p_{i,\mathrm{NC}}^{*}}{\partial v} < 0, \qquad \frac{\partial q_{i,\mathrm{C}}^{*}}{\partial v} = 2\,\frac{\partial q_{i,\mathrm{NC}}^{*}}{\partial v} > 0.$$

Proof. See Appendix I.

According to Proposition 3, under both the non-cooperation and cooperation mechanisms, supply-side uncertainty affects real-time prices and consumption in the same direction. A supply interruption ξ leads to higher real-time prices and lower consumption. As the actual output of VREG increases, real-time prices decrease and consumption increases. Conversely, when VREG output decreases, prices rise and consumption declines.

Although the direction of adjustment is identical across mechanisms, Proposition 3 further shows that the magnitude of these effects under the cooperative mechanism is approximately twice that under the non-cooperative mechanism. In other words, real-time prices and consumption are more sensitive to supply-side uncertainty in the cooperative case. This implies that the coalition responds to uncertainty more actively through stronger price adjustments. As a result, supply-side uncertainty is transmitted more fully to the demand side. Rather than passively bearing imbalance risk, the coalition involves users more directly in the adjustment process, so that supply-side uncertainty is more fully shared between the supply and demand sides.

Proposition 4. *The real-time stage equilibrium decisions both the non-cooperative and cooperative mechanisms differ in both the variability and the expected level of electricity prices and consumption.*

(1) The variances of real-time prices are given by:

$$\mathrm{Var}\big(p_{i,\mathrm{NC}}^{*}\big) = \frac{\phi k_2^2 \gamma^2 \bar{Q}^2}{4(k_2\Lambda + 1)^2}\left(1 - \phi + \frac{\bar{v}^2}{2\alpha + 1}\right) > 0,$$

$$\mathrm{Var}\left(p_{i,\mathrm{C}}^*\right) = \frac{\phi k_2^2 \gamma^2 \bar{Q}^2}{(k_2\Lambda + 1)^2}\left(1 - \phi + \frac{\bar{v}^2}{2\alpha + 1}\right) > 0;$$

(2) Cooperation leads to higher price variance:

$$\mathrm{Var}\left(p_{i,\mathrm{C}}^*\right) - \mathrm{Var}\left(p_{i,\mathrm{NC}}^*\right) = \frac{3\phi k_2^2 \gamma^2 \bar{Q}^2}{4(k_2\Lambda + 1)^2}\left(1 - \phi + \frac{\bar{v}^2}{2\alpha + 1}\right) > 0.$$

(3) Despite the higher volatility, cooperation mechanism reduces the expected price and increases electricity consumption compared to non-cooperation mechanism: $\mathbb{E}(p_{i,\mathrm{C}}^*) < \mathbb{E}(p_{i,\mathrm{NC}}^*)$, $\mathbb{E}(q_{i,\mathrm{C}}^*) > \mathbb{E}(q_{i,\mathrm{NC}}^*)$.

Proof. See Appendix J.

Proposition 4(1) shows that, under both mechanisms, real-time price variance is positively related to the VREG market share and negatively related to forecasting accuracy α. A larger market share implies greater exposure to supply-side uncertainty and thus stronger price fluctuations, while higher forecasting accuracy reduces uncertainty and stabilizes prices. Proposition 4(2) further shows that price variance under cooperation exceeds that under non-cooperation. Moreover, this variance gap widens with the VREG market share and narrows as forecasting accuracy improves. Proposition 4(3) indicates that despite higher price volatility, cooperation leads to a lower expected price and higher expected consumption. Thus, although cooperation increases price responsiveness to uncertainty, it improves outcomes for users in expectation.

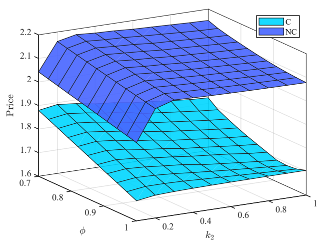

(a) Expected Price

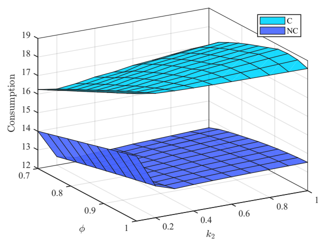

(b) Expected Consumption

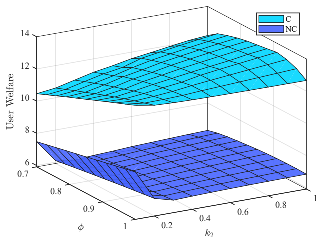

(c) User Welfare

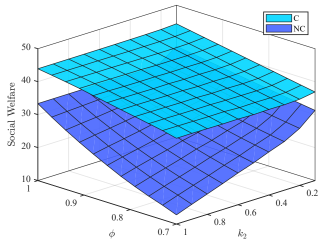

(d) Social Welfare

Figure 5: Impacts of Imbalance Penalty Intensity and Interruption Probability on User-side

Figure 5 further illustrates the numerical results on user welfare and social welfare under the two mechanisms. Consistent with the theoretical results in Proposition 4, although cooperation leads to higher price volatility, it yields a lower expected price and higher expected consumption. As a result, user welfare under cooperation is significantly higher than that under non-cooperation. Moreover, since cooperation also improves supply-side performance, the overall social welfare is increased. These results indicate that cooperation benefits not only the supply side but also the demand side in expectation. The main trade-off lies in slightly higher price fluctuations, while the overall welfare performance is improved.

Proposition 5. *The effects of user dissatisfaction sensitivity η_i and utility intensity l_i on real-time stage equilibrium decisions satisfy*

$$\frac{\partial}{\partial \eta_i} = \bar{q}_i \frac{\partial}{\partial l_i},$$

(1) For each mechanism $m \in \{\mathrm{NC}, \mathrm{C}\}$,

$$\frac{\partial \mathbb{E}(p^*_{i,m})}{\partial \eta_i} > 0, \qquad \frac{\partial \mathbb{E}(q^*_{i,m})}{\partial \eta_i} > 0;$$

(2) Moreover, cooperation mechanisms mitigate these sensitivities compared to non-cooperation mechanisms:

$$\frac{\partial \mathbb{E}(p^*_{i,\mathrm{C}})}{\partial \eta_i} < \frac{\partial \mathbb{E}(p^*_{i,\mathrm{NC}})}{\partial \eta_i}, \qquad \frac{\partial \mathbb{E}(q^*_{i,\mathrm{C}})}{\partial \eta_i} < \frac{\partial \mathbb{E}(q^*_{i,\mathrm{NC}})}{\partial \eta_i}.$$

Proof. See Appendix K.

Proposition 5 first establishes a linear relationship between the effects of dissatisfaction sensitivity η_i and utility intensity l_i. Since their derivatives are proportional, they affect equilibrium outcomes in the same direction, differing only in magnitude. It therefore suffices to discuss one of them. Proposition 5(1) shows that under both cooperative and non-cooperative mechanisms, higher dissatisfaction sensitivity leads to higher expected prices and higher expected consumption. A larger η_i implies that the user is less willing to reduce or shift load, which weakens demand responsiveness and results in higher equilibrium consumption and higher equilibrium prices. By the proportional relationship above, utility intensity l_i has the same directional effect: a stronger valuation of electricity makes the user less willing to reduce demand, thereby sustaining higher consumption and facing higher prices. Proposition 5(2) further shows that these sensitivities are weaker under cooperation. Although user characteristics still influence equilibrium outcomes, cooperation reduces the extent to which prices and consumption differ across users. In other words, cooperation reduces differences in equilibrium prices and consumption across users.

Proposition 6. *When the day-ahead market reaches equilibrium, the influence of predicting* *accuracy α on the expected profits of supply-side participants satisfies the following relationships:*

$$
\begin{aligned}
&(1)\ \frac{\partial \mathbb{E}^*(\pi^{\mathrm{DA}}_{\mathrm{VREG,NC}})}{\partial \alpha} > 0,\ \frac{\partial \mathbb{E}^*(\pi^{\mathrm{DA}}_{\mathrm{ER,NC}})}{\partial \alpha} < 0,\ \frac{\partial \mathbb{E}^*(\pi^{\mathrm{DA}}_{\mathrm{Coa,C}})}{\partial \alpha} > 0;\\
&(2)\ \frac{\partial^2 \mathbb{E}^*(\pi^{\mathrm{DA}}_{\mathrm{VREG,NC}})}{\partial \alpha^2} < 0,\ \frac{\partial^2 \mathbb{E}^*(\pi^{\mathrm{DA}}_{\mathrm{ER,NC}})}{\partial \alpha^2} > 0,\ \frac{\partial^2 \mathbb{E}^*(\pi^{\mathrm{DA}}_{\mathrm{Coa,C}})}{\partial \alpha^2} < 0;\\
&(3)\ \frac{\partial \mathbb{E}^*(\pi^{\mathrm{DA}}_{\mathrm{Coa,C}})}{\partial \alpha} < \frac{\partial \mathbb{E}^*(\pi^{\mathrm{DA}}_{\mathrm{VREG,NC}})}{\partial \alpha} + \frac{\partial \mathbb{E}^*(\pi^{\mathrm{DA}}_{\mathrm{ER,NC}})}{\partial \alpha},\\
&\quad\ \frac{\partial \mathbb{E}^*(\pi^{\mathrm{DA}}_{\mathrm{VREG,C}})}{\partial \alpha} < \frac{\partial \mathbb{E}^*(\pi^{\mathrm{DA}}_{\mathrm{VREG,NC}})}{\partial \alpha},\ \frac{\partial \mathbb{E}^*(\pi^{\mathrm{DA}}_{\mathrm{ER,C}})}{\partial \alpha} > \frac{\partial \mathbb{E}^*(\pi^{\mathrm{DA}}_{\mathrm{ER,NC}})}{\partial \alpha}.
\end{aligned}
$$

Proof. See Appendix L.

Proposition 6(1) shows that in the day-ahead market, the expected profits of both the VREG and the coalition are positively correlated with predicting accuracy α, while the ER's expected profit is negatively correlated. Specifically, improving predicting accuracy means that deviation distributions converge toward the mean, reducing system imbalance, thereby lowering the VREG's commitment risk and enhancing the credibility of its day-ahead generation commitments. This acts as a direct positive incentive for both the VREG and the coalition. However, for the ER, improved predicting accuracy reduces opportunities to profit from real-time demand response, thus suppressing its profit potential. Proposition 6(2) indicates that, regardless of the mechanism, the marginal benefit of improving predicting accuracy for the VREG exhibits diminishing returns, while its marginal impact on the ER decreases. Additionally, Proposition 6(3) shows that, compared with the non-cooperative mechanism, the cooperative mechanism reduces the overall benefits of improving predicting accuracy. Specifically, under cooperation, the marginal gains for the ER increase, whereas those for the VREG decrease.

5.2. Case Study: Evidence from the German Electricity Market

To examine the applicability of the model in a real market environment, we conduct a case study using 15-minute resolution data for Germany in December 2024 obtained from ENTSO-E. This period coincides with a typical "Dunkelflaute" episode, during which VRE generation declined markedly while system demand remained elevated, resulting in a pronounced supply–demand gap. Figure 6 illustrates the temporal dynamics of supply–demand conditions and market prices. As shown in Figure 6(a), both VRE output and system demand exhibit substantial fluctuations over time. Notably, during December 11–14, VRE generation declined sharply and remained at a persistently low level, whereas system demand did not decrease proportionally. This divergence led to a pronounced imbalance between supply and demand. Figure 6(b) reports the corresponding movements of day-ahead and imbalance prices. During periods of reduced VRE output, day-ahead prices increased markedly. More importantly, imbalance prices displayed significantly higher volatility and more extreme realizations, indicating that imbalance settlement risk intensifies under conditions of

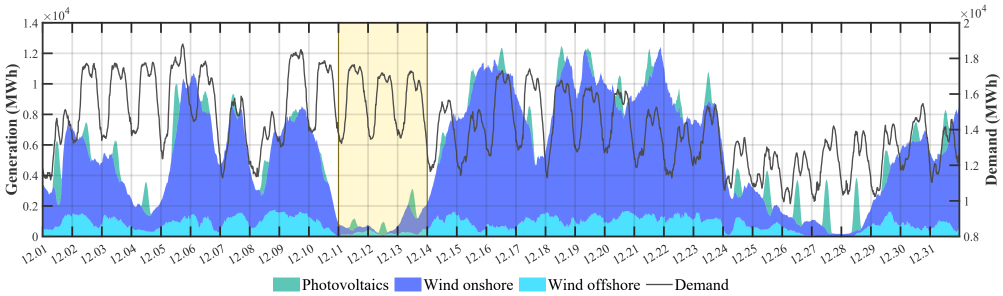

(a) VRE Generation and System Demand

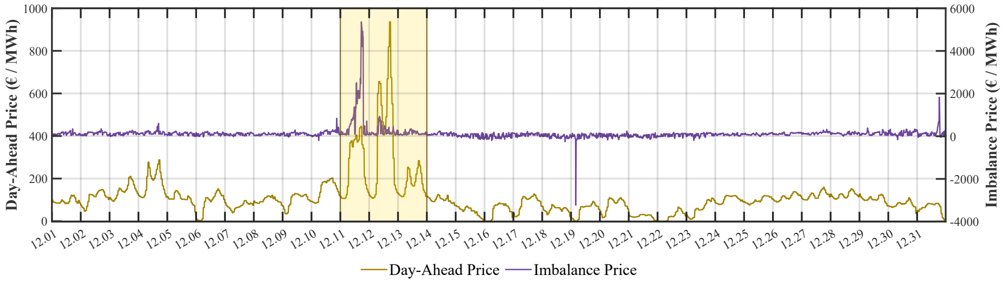

(b) Day-Ahead and Imbalance Prices

Figure 6: Supply–Demand and Electricity Price Fluctuations

supply shortfall. Accordingly, the sample exhibits multi-source uncertainty characterized by concurrent supply-side shocks and demand-side fluctuations, which aligns closely with the theoretical framework developed in this study.

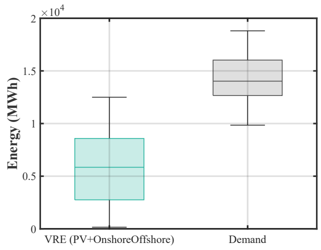

(a) Generation and Demand

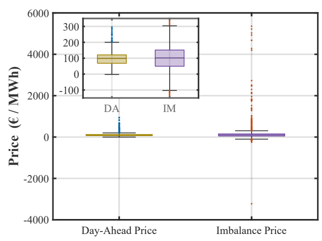

(b) Electricity Prices

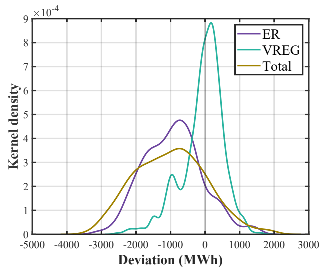

(c) Market Deviations

Figure 7: Distributional Characteristics of Supply–Demand, Electricity Prices and Market Deviations

Figure 7 presents the distributional characteristics of supply–demand conditions and market prices. As shown in Figure 7(a), the variability of VRE output is substantially larger relative to system demand, reflecting the inherent intermittency of renewable generation. Figure 7(b) further indicates that the imbalance price exhibits significantly greater dispersion and more extreme realizations than the day-ahead price, implying that real-time settlement outcomes are highly sensitive to supply–demand deviations. Figure 7(c) reports the distributional properties of market deviations. Both the total deviation and the ER's deviation are predominantly concentrated in the negative region, indicating that realized consumption frequently exceeded day-ahead procurement levels, thereby leading to supply shortfalls in real time. In contrast, VRE deviations display an approximately symmetric distribution around zero, which is consistent with the symmetric Beta specification introduced in Section 3.2.1. Overall, the empirical evidence suggests that multi-source uncertainty generates substantial imbalance exposure in practice, particularly through amplified real-time price volatility and asymmetric deviation realizations.

Building on the documented evidence of multi-source uncertainty and elevated imbalance exposure, we next compare the cooperative and non-cooperative mechanisms. Figure 8(a) presents the distribution of total deviation under both mechanisms. Under non-cooperation, the distribution is predominantly concentrated in the negative region, indicating that realized consumption frequently exceeded day-ahead procurement levels, thereby generating systematic real-time supply deficits. Under cooperation, the entire distribution shifts toward zero, substantially mitigating the structural negative bias in deviations. Figure 8(b) reports the corresponding tail risk measures. In the left tail, both $\mathrm{VaR}_{0.05}$ and $\mathrm{CVaR}^{-}_{0.05}$ move closer to zero under cooperation, implying a reduction in extreme negative deviations. In the right tail, $\mathrm{VaR}_{0.95}$ and $\mathrm{CVaR}^{+}_{0.95}$ increase moderately, reflecting a rebalancing of the deviation structure toward greater symmetry. Overall, cooperation does not eliminate deviations. Instead, it reduces the structural deficit tendency and shifts the distribution toward a more balanced configuration around zero.

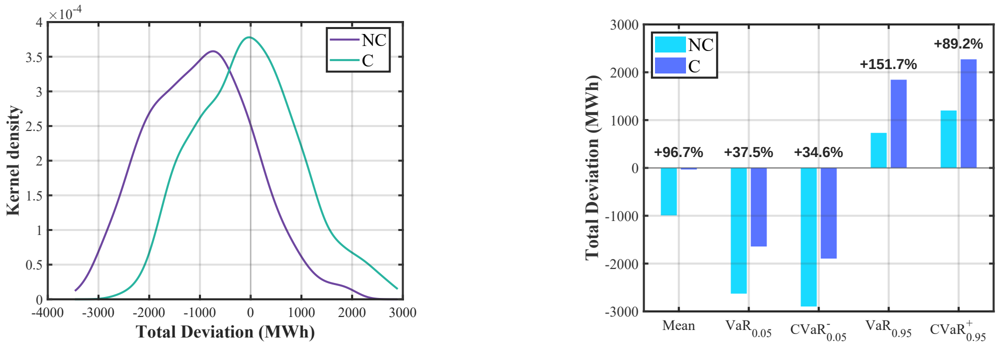

(a) Kernel Density

(b) Summary Statistics

Figure 8: Total Deviation under Cooperation and Non-Cooperation.

Notes: VaR_α is the α-quantile and CVaR_α is Conditional Value-at-Risk; superscripts $-/+$ indicate left/right tails; Change (%)= $(C - NC)/|NC|$.

Figure 9 further examines the magnitude of total deviation measured in absolute terms. As shown in Figure 9(a), under cooperation, the distribution of absolute deviations becomes more concentrated around zero, with a pronounced reduction in the upper tail density. Figure 9(b) reports the corresponding summary statistics. Cooperation reduces the mean by 29.2%, $\mathrm{VaR}_{0.95}$ by 22.8%, and $\mathrm{CVaR}^{+}_{0.95}$ by 19.0%. These results indicate that cooperation not only lowers the average imbalance magnitude but also compresses extreme deviation risk in the right tail.

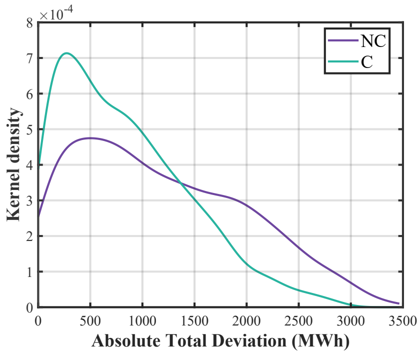

(a) Kernel Density

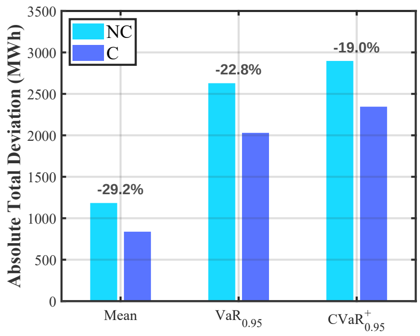

(b) Summary Statistics

Figure 9: Absolute Total Deviation under Cooperation and Non-Cooperation

Table 1: Imbalance Settlement and Coalition Profit

Metric	NC	C	Change (%)
Total Imbalance Settlement ($\times 10^5$ €)			
Mean	-1.35	-0.18	86.7
$\mathrm{VaR}_{0.05}$	-4.38	-2.48	43.3
$\mathrm{CVaR}^{-}_{0.05}$	-11.98	-4.68	61.0
$\mathrm{VaR}_{0.95}$	0.92	1.96	111.7
$\mathrm{CVaR}^{+}_{0.95}$	2.35	3.07	30.5
Absolute Total Imbalance Settlement ($\times 10^5$ €)			
Mean	1.70	1.06	-37.6
$\mathrm{VaR}_{0.95}$	4.44	2.88	-35.1
$\mathrm{CVaR}^{+}_{0.95}$	12.60	5.30	-57.9
Coalition Profit ($\times 10^6$ €)			
Mean	3.86	3.99	3.4
$\mathrm{VaR}_{0.05}$	2.59	2.66	2.7
$\mathrm{CVaR}^{-}_{0.05}$	-1.11	-0.72	35.2
$\mathrm{VaR}_{0.95}$	5.63	5.74	1.9
$\mathrm{CVaR}^{+}_{0.95}$	5.88	5.96	1.4

Improvements in deviation magnitude translate directly into changes in imbalance settlements. Table 1 reports the distribution of total imbalance settlement under the two mechanisms. Under cooperation, the magnitude of negative settlements decreases substantially and the overall distribution shifts toward zero, indicating a mitigation of systematic settlement exposure. For the absolute imbalance settlement, cooperation reduces the mean by 37.6%, $\mathrm{VaR}_{0.95}$ by 35.1%, and $\mathrm{CVaR}^{+}_{0.95}$ by 57.9%. These results demonstrate that cooperation significantly attenuates tail settlement exposure, particularly under extreme risk realizations. We further compare the supply-side coalition profit while holding demand-side welfare constant. Cooperation increases the coalition's average profit by 3.4% and markedly improves left-tail risk, with $\mathrm{CVaR}^{-}_{0.05}$ improving by 35.2%. This indicates that, conditional on unchanged consumption and user welfare, cooperation not only enhances expected returns but also substantially reduces extreme loss risk. Because demand-side welfare remains invariant, the increase in coalition profit is equivalent to an improvement in social welfare.

Taken together, the empirical evidence confirms that real-world markets exhibit pronounced multi-source uncertainty accompanied by significant imbalance price risk; the cooperative mechanism compresses system-wide deviation magnitude, alleviates tail exposure, and improves both supply-side profitability and overall welfare.

6. Extensions

6.1. Incomplete Demand Response

In the original model, demand response is assumed to be complete. Specifically, users fully implement the adjustment targeted by the ER's real-time pricing, and the ER correctly anticipates this response. In practice, this assumption may not hold. First, demand response may be incomplete—users implement only part of the intended load adjustment. Second, even if the ER recognizes that the response is incomplete, it may not accurately observe or infer the actual response level. An inconsistency may therefore arise between the response level perceived by the ER and the response level actually implemented by users. To capture these features, we extend the model along two dimensions: (i) incomplete user response, and (ii) discrepancies between the ER's perceived and realized user responses. Specifically, we introduce two parameters: $\hat{\rho} \in [0, 1]$: the response level perceived by the ER; $\rho \in [0, 1]$: the response level actually implemented by users.

We first define a baseline consumption corresponding to the operating state in which no supply-side uncertainty arises, that is, the VREG's realized output equals its day-ahead commitment. In this case, according to Theorems 1 and 3, the ER sets the baseline price p_i^{base}, and user i's baseline consumption q_i^{base} is given by

$$p_i^{base} = \frac{1}{2b_i} + \frac{k_1(\theta\bar{Q} - Q_{VREG}^C) - k_2(2\theta\bar{Q} - \bar{Q})}{2(k_2\Lambda + 1)},$$

$$q_i^{base} = \bar{q}_i(1 - b_i p_i^{base}) + \varepsilon_i.$$

Accordingly, the total baseline demand is given by $Q^{base} = \sum_{i=1}^{N} q_i^{base}$. Under complete demand response, the adjustment is $\Delta q_i = q_i^* - q_i^{base}$, where q_i^* denotes the optimal consumption derived in the original model. Under incomplete demand response, only a fraction of this adjustment is implemented. The consumption perceived by the ER is $q_i^{per} = q_i^{base} + \hat{\rho}\Delta q_i$, while the actual consumption is $q_i^{act} = q_i^{base} + \rho\Delta q_i$.

Theorem 6. *Under incomplete demand response, the equilibrium real-time prices faced by users* *under the non-cooperative and cooperative mechanisms are given by*

$$p_{i,\mathrm{NC}}^{\mathrm{IDR}\,*} = \frac{\hat{\rho}\bar{q}_i + (1-\hat{\rho})q_i^{base}}{2\hat{\rho}\bar{q}_i b_i} + \frac{\Theta_1 - k_2(Q_{\mathrm{VREG}}^{\mathrm{A}} - Q_{\mathrm{VREG}}^{\mathrm{C}})}{2(1+\hat{\rho}k_2\Lambda)},$$

$$p_{i,\mathrm{C}}^{\mathrm{IDR}*} = \frac{\hat{\rho}\bar{q}_i + (1-\hat{\rho})q_i^{base}}{2\hat{\rho}\bar{q}_i b_i} + \frac{\Theta_1 - 2k_2(Q_{\mathrm{VREG}}^{\mathrm{A}} - Q_{\mathrm{VREG}}^{\mathrm{C}})}{2(1+\hat{\rho}k_2\Lambda)}.$$

where $\Theta_1 = k_1(\theta\bar{Q} - Q_{\mathrm{VREG}}^{\mathrm{C}}) - k_2(2\theta\bar{Q} - \hat{\rho}\bar{Q}) + (1-\hat{\rho})k_2 Q^{base}$.

Proof. See Appendix M.

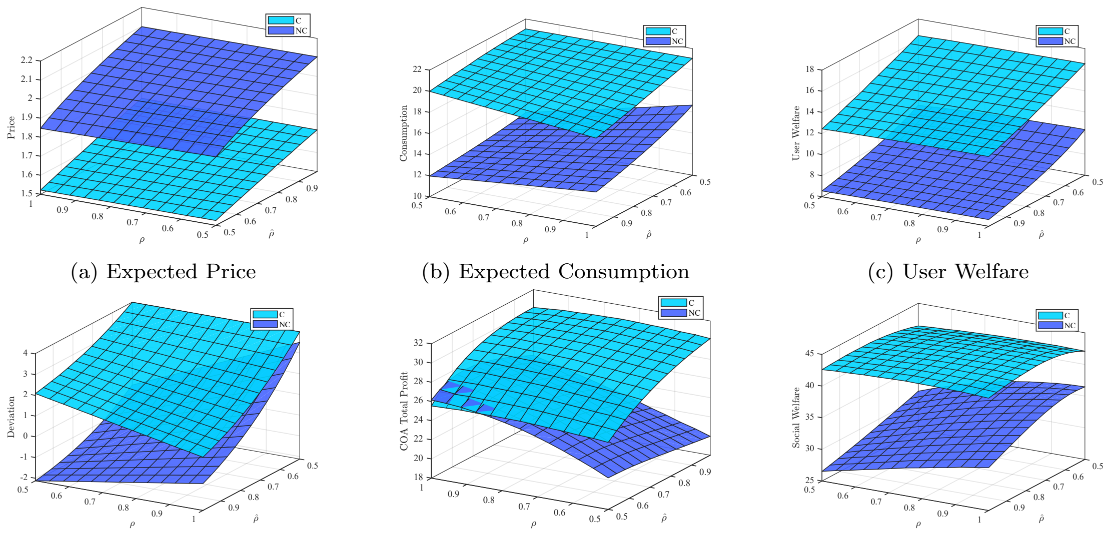

(a) Expected Price (b) Expected Consumption (c) User Welfare

(d) Total Deviation (e) COA Total Profit (f) Social Welfare

Figure 10: Effects of Demand Response Level on Market Outcomes

The numerical simulations reported in Figure 10 reveal the structural effects induced by changes in the degree of demand response. From the user perspective, as the actual response level ρ increases, users become more sensitive to price signals. As shown in Figure 10(a) and (b), higher ρ leads to higher expected prices and lower expected consumption. Consequently, user welfare declines, as illustrated in Figure 10(c). From the supply-side and system perspective, however, an increase in demand response capability plays a stabilizing role. Since users respond more effectively to price signals, supply–demand matching improves and overall system deviations are significantly reduced, as shown in Figure 10(d). At the same time, supply-side profit performance improves, as reflected in Figure 10(e). In other words, stronger demand response helps absorb supply-side shocks, alleviates real-time adjustment pressure on generators, and enhances profit stability. Furthermore, the misperception effect differs markedly across mechanisms. Under the non-cooperative mechanism, when the ER overestimates or underestimates the response capability (i.e., $\hat{\rho} > \rho$ or $\hat{\rho} < \rho$), overall market deviations increase significantly. This indicates that the non-cooperative structure is highly sensitive to perception errors, and both overestimation and underestimation amplify system fluctuations. By contrast, under the cooperative mechanism, deviations are less sensitive to misperception. Even when cognitive bias exists, its impact on system stability is mitigated. Overall, although stronger demand response reduces user welfare, its positive effects on supply-side performance and system efficiency dominate, resulting in higher social welfare, as shown in Figure 10(f). To maintain user participation while enhancing demand response capability, subsidy or profit-redistribution schemes may be considered to return part of the efficiency gains to users, thereby achieving a dynamic balance between efficiency and fairness.

6.2. Capacity Constraint of FPG

In the original model, system flexibility is jointly provided by FPG real-time adjustment and price-based demand response. Demand response is naturally bounded below by users' minimum consumption $\underline{q}_i$. As characterized in Equations (9) and (20), consumption reaches this minimum when the price attains its upper bound $\bar{p}_i = (\bar{q}_i - \underline{q}_i)/(b_i\bar{q}_i)$. By contrast, FPG was assumed to possess unlimited capacity. We now relax this assumption by introducing capacity constraints: $-\underline{Q}_{\text{FPG}} \leq Q_{\text{FPG}} \leq \bar{Q}_{\text{FPG}}$, where $\bar{Q}_{\text{FPG}}$ denotes the maximum generation capacity and $\underline{Q}_{\text{FPG}}$ represents the maximum absorption capability.

When system flexibility is finite, two types of extreme imbalance may arise: excess supply and supply shortage. Excess supply beyond flexibility leads to VRE being curtailed or spilled. Since the marginal cost of VRE is close to zero, the associated economic loss is negligible and system security is not jeopardized. In contrast, supply shortage may threaten system reliability. In such cases, the SO must resort to non-market interventions, such as involuntary load shedding, to maintain grid stability. We therefore focus on this case.

A residual demand gap occurs only after both flexibility sources—demand response and FPG capacity—are fully exhausted. We define the involuntary load shedding amount as

$$L = \max\left(Q_{\min} - S^{\text{A}} - \bar{Q}_{\text{FPG}},\, 0\right).$$

The value of L determines the system operation mechanism and market settlement rule, leading to the following two cases.

Case 1 ($L = 0$). When $\bar{Q}_{\text{FPG}} \geq Q_{\min} - S^{\text{A}}$, the system reduces to the original model analyzed in the previous sections. The imbalance pricing mechanism alone restores supply–demand balance, and no involuntary load shedding occurs.

Case 2 ($L > 0$). When $\bar{Q}_{\text{FPG}} < Q_{\min} - S^{\text{A}}$, even after demand is reduced to $Q_{\min}$ and FPG operates at its capacity limit $\bar{Q}_{\text{FPG}}$, the supply deficit is only partially offset, with the remaining portion left unserved. For the compensated portion, imbalance settlement is based on the actual FPG dispatch $\bar{Q}_{\text{FPG}}$, and the imbalance price reaches its upper bound $\bar{w}^{IM} = k_1 Q_{\text{TEG}} + k_2\bar{Q}_{\text{FPG}}$.

The settlement quantity is allocated proportionally between VREG and ER according to their respective deviation contributions. Specifically, VREG and ER bear

$$\frac{\Delta Q_{\text{VREG}}}{Q_{\min} - S^{\text{A}}}\,\bar{Q}_{\text{FPG}}, \qquad \frac{\Delta Q_{\text{ER}}}{Q_{\min} - S^{\text{A}}}\,\bar{Q}_{\text{FPG}}.$$

For the uncompensated portion, the SO must implement involuntary load shedding to maintain system reliability. Users are indexed in ascending order of marginal outage cost, so that users with lower outage costs are curtailed first. There exists a unique integer M such that $\sum_{i=1}^{M-1} \underline{q}_i < L \le \sum_{i=1}^{M} \underline{q}_i$. Thus, the first M users are curtailed to eliminate the residual demand gap L. As L increases, load shedding extends to users with higher marginal outage costs, so that the marginal outage loss is increasing in L. Consequently, the total outage loss is an increasing and convex function of L. We therefore approximate the total involuntary outage loss by μL^2, where $\mu > 0$ denotes the loss coefficient. This loss is shared between ER and VREG in proportions ω and $1-\omega$, respectively. The real-time equilibrium under capacity constraints is characterized as follows.

Theorem 7. *Under FPG capacity constraints, for each mechanism $m \in \{\text{NC}, \text{C}\}$, the real-time equilibrium price $p_{i,m}^{cap,*}$ and consumption $q_{i,m}^{cap,*}$ are given by*

$$p_{i,m}^{cap,*} = \begin{cases} p_{i,m}^{*}, & L = 0, \\ \bar{p}_i, & L > 0, \end{cases} \qquad q_{i,m}^{cap,*} = \begin{cases} q_{i,m}^{*}, & L = 0, \\ \underline{q}_i, & L > 0. \end{cases}$$

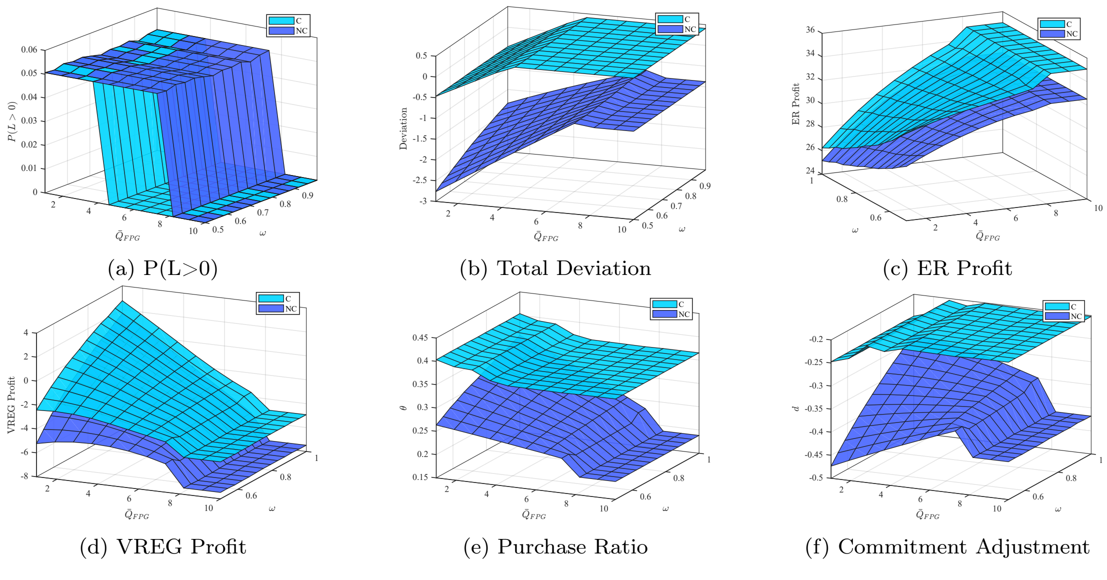

Figure 11: Effects of Capacity Constraint on Market Outcomes

We then numerically compute the day-ahead equilibria under both mechanisms to examine how the introduction of capacity constraints alters market outcomes, as shown in Figure 11. First, increasing the FPG capacity limit $\bar{Q}_{\text{FPG}}$ or adopting the cooperative mechanism lowers the probability that $L > 0$, thereby reducing the likelihood of involuntary load shedding. When $\bar{Q}_{\text{FPG}}$ is sufficiently large, market-based flexibility alone is able to restore supply–demand balance. Hence, expanding FPG capacity improves system reliability. In addition, a higher $\bar{Q}_{\text{FPG}}$ reduces overall supply–demand deviations, with the effect being particularly pronounced under the non-cooperative mechanism. Second, the welfare effects differ across market participants. Users and the ER benefit more from capacity expansion. Users face a lower outage risk, while the ER's profit performance improves significantly as flexibility increases. By contrast, the impact on the VREG is limited. When $\bar{Q}_{\text{FPG}}$ is small, the allocation of outage losses becomes crucial under the non-cooperative mechanism. A higher ω, meaning that the ER bears a larger share of the outage loss μL^2, induces both the ER and the VREG to adopt higher commitment levels in the day-ahead stage. This strengthens forward contracting incentives, reduces system deviations, lowers the probability of $L > 0$, and improves user welfare and overall market performance. Overall, under more realistic flexibility limitations, the original model may underestimate the value of the cooperative mechanism.

7. Conclusion

This study focuses on the supply–demand balancing challenges in electricity markets characterized by imbalance pricing and multi-source uncertainty. Based on the two-stage structure of the day-ahead market and the real-time market, it models and solves game interactions among the VREG, the ER, and users under non-cooperative and cooperative mechanisms. The key findings are summarized as follows.

- Cooperation improves overall market performance. It increases the profits of supply-side participants and raises user welfare, so social welfare is higher than under non-cooperation. It also reduces market deviation and lowers the likelihood of extreme imbalance settlement.

- Cooperation affects equilibrium outcomes asymmetrically. When VREG market share is small, cooperation encourages higher generation commitments. When VREG market share is large, cooperation induces more conservative commitments to contain systemic risk.

- Under multi-source uncertainty, cooperation leads to stronger price-based adjustment on the demand side, which results in higher retail price volatility and greater risk exposure for users. Even so, retail prices remain within regulatory bounds in our setting. Cooperation delivers lower expect retail prices, higher expect consumption, and higher expect user welfare. We also find that cooperation moderates prices disparities across heterogeneous users compared with non-cooperation, suggesting a more equitable outcome.

- Forecast accuracy matters for both efficiency and profitability. Improving forecast accuracy reduces deviations, stabilizes retail prices, and increases the profits of VREG and the coalition, although the marginal benefit diminishes as accuracy becomes high. Finally, cooperation weakens but does not eliminate VREG's incentive to improve forecasting accuracy, because risk sharing reduces the marginal gain from additional accuracy improvements.

The findings provide managerial insights for different stakeholders in the electricity market:

- **For the ER:** Electricity retailers should first assess users' willingness to provide demand response and then adjust pricing and contract design accordingly. In practice, offering a menu of retail contracts can better match heterogeneous risk tolerance, allowing users who are willing to bear more price risk to access lower expected prices. At the same time, retail pricing, including dynamic pricing, should remain within regulatory bounds and avoid extreme levels that may harm customer trust and long-term business performance.
- **For the VREG:** In the short run, cooperation can be a practical option because it reduces imbalance exposure without requiring large upfront investment. In the long run, however, VREG should not rely on cooperation alone. They should continue improving forecasting quality and plan for physical flexibility such as energy storage, since these capabilities remain essential for sustained performance and risk control.
- **For the coalition:** A coalition can create additional value through coordinated decisions and risk sharing, but it should avoid becoming dependent on this arrangement. Members should keep investing in forecast-quality improvements and physical flexibility to strengthen long-term competitiveness and system reliability. Moreover, since cooperation may increase retail price volatility, the coalition can allocate a small share of the cooperation gains to support users facing extreme conditions, which helps reduce short-term hardship and improves the acceptability of cooperation.
- **For regulators:** Regulators may allow a cooperating coalition to act as the responsible entity for imbalance settlement, but this permission should come with clear requirements. In particular, the coalition should adopt a transparent internal settlement rule, and benefit sharing should explicitly account for each member's deviation contribution and forecasting performance. Regulators can further strengthen incentives by adjusting imbalance charges or collateral requirements based on participants' sustained imbalance outcomes, so that persistent underperformance leads to higher effective charges. Part of the revenue from imbalance settlement can also be used to support verified investments that improve forecasting quality. Finally, given the potential increase in retail price volatility under cooperation, regulators should strictly enforce price caps and floors, require clear risk disclosure, and set basic compliance rules for retail contract design and sales practices.

Future research could expand this framework in several directions. First, incorporating flexibility resources such as energy storage and virtual power plants could enhance supply–demand balancing capabilities. Second, future work could explore the adaptability of imbalance pricing mechanisms in different market environments, aiming to design more efficient and fair regulatory strategies. In addition, since carbon markets and policy factors significantly influence market behavior, integrating carbon emission constraints and pricing mechanisms into the analysis would better support the green energy transition and policy formulation.

CRediT authorship contribution statement

Yeming Dai: Conceptualization, Methodology, Writing – review & editing, Supervision, Funding acquisition. Rongqing Yin: Formal analysis, Validation, Writing – original draft, Visualization, Software. Mingming Leng: Supervision, Writing – review & editing.

Declaration of competing interest

The authors declare that they have no known competing financial interests or personal relationships that could have appeared to influence the work reported in this paper.

Acknowledgments

This work was supported by the National Natural Science Foundation of China (No. 72371139), the General Research Fund (GRF) of the Hong Kong Research Grants Council (No. LU13500025).

Declaration of Generative AI and AI-assisted technologies in the writing process

During the preparation of this work the author(s) used ChatGPT in order to improve language and readability. After using this tool/service, the author(s) reviewed and edited the content as needed and take(s) full responsibility for the content of the publication.

References

[1] S. Reed, M. Eddy, Dark doldrums overshadow europe's energy markets, New York Times (2024).

[2] J. Ambrose, "Blackouts can happen anywhere": How power systems worldwide can collapse, The Guardian (2025).

[3] Y. Ghiassi-Farrokhfal, R. Belo, M. R. Hesamzadeh, D. Bunn, Optimal electricity imbalance pricing for the emerging penetration of renewable and low-cost generators, Manufacturing & Service Operations Management 25 (2023) 1966–1983. doi:10.1287/msom.2021.0555.

[4] P. Shinde, M. R. Hesamzadeh, P. Date, D. W. Bunn, Optimal dispatch in a balancing market with intermittent renewable generation, IEEE Transactions on Power Systems 36 (2021) 865–878. doi:10.1109/TPWRS.2020.3014515.

[5] ENTSO-E, Explanatory document to all tsos' proposal to further specify and harmonise imbalance settlement in accordance with article 52(2) of commission regulation (eu) 2017/2195 (2018).

[6] N. Gohdes, P. Simshauser, C. Wilson, Renewable investments, hybridised markets and the energy crisis: Optimising the CfD-merchant revenue mix, Energy Economics 125 (2023) 106824. doi:10.1016/j.eneco.2023.106824.

[7] K. N. Hasan, R. Preece, J. V. Milanović, Existing approaches and trends in uncertainty modelling and probabilistic stability analysis of power systems with renewable generation, Renewable and Sustainable Energy Reviews 101 (2019) 168–180. doi:10.1016/j.rser.2018.10.027.

[8] M. Al-Gwaiz, X. Chao, O. Q. Wu, Understanding how generation flexibility and renewable energy affect power market competition, Manufacturing & Service Operations Management 19 (2017) 114–131. doi:10.1287/msom.2016.0595.

[9] S. Aflaki, S. Netessine, Strategic investment in renewable energy sources: The effect of supply intermittency, Manufacturing & Service Operations Management 19 (2017) 489–507. doi:10.1287/msom.2017.0621.

[10] S. S. Gharehveran, S. Ghassemzadeh, N. Rostami, Two-stage resilience-constrained planning of coupled multi-energy microgrids in the presence of battery energy storages, Sustainable Cities and Society 83 (2022) 103952. doi:10.1016/j.scs.2022.103952.

[11] H. Lv, Q. Wu, H. Ren, Q. Li, W. Zhou, A two-stage decision-making approach for optimal design and operation of integrated energy systems considering multiple uncertainties and diverse resilience needs, Energy 305 (2024) 132375. doi:10.1016/j.energy.2024.132375.

[12] H. Ren, Z. Jiang, Q. Wu, Q. Li, Y. Yang, Integrated optimization of a regional integrated energy system with thermal energy storage considering both resilience and reliability, Energy 261 (2022) 125333. doi:10.1016/j.energy.2022.125333.

[13] H. Panahi, F. Sabouhi, A. Bozorgi-Amiri, S. F. Ghaderi, A data-driven optimization model for renewable electricity supply chain design, Renewable and Sustainable Energy Reviews 202 (2024) 114618. doi:10.1016/j.rser.2024.114618.

[14] J. Feng, Z. Hu, X. Duan, S. Cai, P. Zhang, A multi-stage DRO-SDDP approach for planning multi-type energy storage systems and flexible resources in high-penetration renewable power systems, IEEE Transactions on Industry Applications (2025) 1–14doi:10.1109/TIA.2025.3549390.

[15] Y. Xie, Y. Xu, Z. Yi, S. Lin, B. Zhang, X. Zhu, A hybrid stochastic-robust planning approach for flexible devices in an islanded integrated energy system considering multiple uncertainties and demand response, IEEE Transactions on Industry Applications (2025) 1–15doi:10.1109/TIA.2025.3561764.

[16] G. G. Parker, B. Tan, O. Kazan, Electric power industry: Operational and public policy challenges and opportunities, Production and Operations Management 28 (2019) 2738–2777. doi:10.1111/poms.13068.

[17] J. Lin, C. Gao, J. Zeng, F. Han, Stackelberg–nash asymmetric bargaining-based scheduling optimization and revenue allocation for multi-operator regional integrated energy systems considering competition–cooperation relationships and source–load uncertainties, Energy 291 (2024) 130262. doi:10.1016/j.energy.2024.130262.

[18] K. Zhou, Y. Chu, R. Hu, Energy supply–demand interaction model integrating uncertainty forecasting and peer-to-peer energy trading, Energy 285 (2023) 129436. doi:10.1016/j.energy.2023.129436.

[19] L. Vandezande, L. Meeus, R. Belmans, M. Saguan, J.-M. Glachant, Well-functioning balancing markets: A prerequisite for wind power integration, Energy Policy 38 (2010) 3146–3154. doi:10.1016/j.enpol.2009.07.034.

[20] R. A. C. van der Veen, A. Abbasy, R. A. Hakvoort, Agent-based analysis of the impact of the imbalance pricing mechanism on market behavior in electricity balancing markets, Energy Economics 34 (2012) 874–881. doi:10.1016/j.eneco.2012.04.001.

[21] D. W. Bunn, S. O. E. Kermer, Statistical arbitrage and information flow in an electricity balancing market, The Energy Journal 42 (2021) 19–40. doi:10.5547/01956574.42.5.dbun.

[22] N. Sunar, J. R. Birge, Strategic commitment to a production schedule with uncertain supply and demand: Renewable energy in day-ahead electricity markets, Management Science 65 (2019) 714–734. doi:10.1287/mnsc.2017.2961.

[23] S. Clò, E. Fumagalli, The effect of price regulation on energy imbalances: A difference-in-differences design, Energy Economics 81 (2019) 754–764. doi:10.1016/j.eneco.2019.05.008.

[24] S. Yamujala, K. Das, M. J. Koivisto, M. Gupta, P. Kanellas, Requirements of future european balancing markets: Insights into imbalance volumes and generation availability, in: IET Conference Proceedings, 2023, pp. 282–288. doi:10.1049/icp.2023.2749.

[25] H. Chen, J. Li, N. O'Leary, J. Shao, Examining the drivers of the imbalance price: Insights from the balancing mechanism in the United Kingdom, Journal of Environmental Management 371 (2024) 123239. doi:10.1016/j.jenvman.2024.123239.

[26] G. P. Cachon, M. A. Lariviere, Contracting to assure supply: How to share demand forecasts in a supply chain, Management Science 47 (2001) 629–646. doi:10.1287/mnsc.47.5.629.10486.

[27] G. P. Cachon, M. A. Lariviere, Supply chain coordination with revenue-sharing contracts: Strengths and limitations, Management Science 51 (2005) 30–44. doi:10.1287/mnsc.1040.0215.

[28] B. C. Giri, S. Bardhan, T. Maiti, Coordinating a three-layer supply chain with uncertain demand and random yield, International Journal of Production Research 54 (2016) 2499–2518. doi:10.1080/00207543.2015.1119324.

[29] F. El Ouardighi, K. Kogan, Dynamic conformance and design quality in a supply chain: An

assessment of contracts' coordinating power, Annals of Operations Research 211 (2013) 137–166. doi:10.1007/s10479-013-1414-4.

[30] S. Y. Tang, P. Kouvelis, Pay-back-revenue-sharing contract in coordinating supply chains with random yield, Production and Operations Management 23 (2014) 2089–2102. doi:10.1111/poms.12240.

[31] Z. Zhu, L. Kong, J. Xie, J. Li, B. Cao, Contract coordination optimization of a multi-power supplier–single dominant grid supply chain in a hybrid electricity market, Industrial Management & Data Systems 119 (2019) 1861–1887. doi:10.1108/IMDS-08-2018-0340.

[32] Z. Zhu, L. Kong, G. Aisaiti, M. Song, Z. Mi, Pricing contract design of a multi-supplier–multi-retailer supply chain in a hybrid electricity market, Industrial Management & Data Systems 121 (2021) 1522–1551. doi:10.1108/IMDS-09-2020-0543.

[33] L. Kong, Z. Zhu, J. Xie, J. Li, Y. Chen, Multilateral agreement contract optimization of renewable energy power grid-connecting under uncertain supply and market demand, Computers & Industrial Engineering 135 (2019) 689–701. doi:10.1016/j.cie.2019.06.016.

[34] X. Lei, H. Yu, Z. Shao, L. Jian, Optimal bidding and coordinating strategy for maximal marginal revenue due to V2G operation: Distribution system operator as a key player in China's uncertain electricity markets, Energy 283 (2023) 128354. doi:10.1016/j.energy.2023.128354.

[35] Y. Li, J. Li, J. He, S. Zhang, The real-time pricing optimization model of smart grid based on the utility function of the logistic function, Energy 224 (2021) 120172. doi:10.1016/j.energy.2021.120172.

[36] D. Qu, J. Li, X. Ma, Distributed real-time pricing of smart grid considering individual differences, Omega 127 (2024) 103109. doi:10.1016/j.omega.2024.103109.

[37] L. Wen, K. Zhou, J. Li, S. Wang, Modified deep learning and reinforcement learning for an incentive-based demand response model, Energy 205 (2020) 118019. doi:10.1016/j.energy.2020.118019.

[38] A. Mas-Colell, M. D. Whinston, J. R. Green, Microeconomic Theory, Oxford University Press, 2021.

[39] L. S. Shapley, A value for n-person games, in: H. W. Kuhn (Ed.), Classics in Game Theory, Princeton University Press, 2020, pp. 69–79. doi:10.1515/9781400829156-012.

[40] K. Ito, M. Reguant, Sequential markets, market power, and arbitrage, American Economic Review 106 (2016) 1921–1957. doi:10.1257/aer.20141529.